NAVAL POSTGRADUATE SCHOOL

MONTEREY, CALIFORNIA

THESIS

REMOTE SENSING OF SULFUR DIOXIDE (SO$_2$) USING THE LINEATE IMAGING NEAR-ULTRAVIOLET SPECTROMETER (LINUS)

by

Sing Soong Khoo

March 2005

Thesis Advisor:	Richard M. Harkins
Co-Advisor:	Richard C. Olsen

Approved for public released; distribution is unlimited

THIS PAGE INTENTIONALLY LEFT BLANK

REPORT DOCUMENTATION PAGE	*Form Approved OMB No. 0704-0188*

Public reporting burden for this collection of information is estimated to average 1 hour per response, including the time for reviewing instruction, searching existing data sources, gathering and maintaining the data needed, and completing and reviewing the collection of information. Send comments regarding this burden estimate or any other aspect of this collection of information, including suggestions for reducing this burden, to Washington headquarters Services, Directorate for Information Operations and Reports, 1215 Jefferson Davis Highway, Suite 1204, Arlington, VA 22202-4302, and to the Office of Management and Budget, Paperwork Reduction Project (0704-0188) Washington DC 20503.

1. AGENCY USE ONLY *(Leave blank)*	2. REPORT DATE March 2005	3. REPORT TYPE AND DATES COVERED Master's Thesis

4. TITLE AND SUBTITLE: Remote Sensing of Sulfur Dioxide (SO_2) using the Lineate Imaging Near-Ultraviolet Spectrometer (LINUS)	5. FUNDING NUMBERS
6. AUTHOR(S)	

7. PERFORMING ORGANIZATION NAME(S) AND ADDRESS(ES) Naval Postgraduate School Monterey, CA 93943-5000	8. PERFORMING ORGANIZATION REPORT NUMBER

9. SPONSORING /MONITORING AGENCY NAME(S) AND ADDRESS(ES) N/A	10. SPONSORING/MONITORING AGENCY REPORT NUMBER

11. SUPPLEMENTARY NOTES The views expressed in this thesis are those of the author and do not reflect the official policy or position of the Department of Defense or the U.S. Government.

12a. DISTRIBUTION / AVAILABILITY STATEMENT Approved for public released; distribution is unlimited	12b. DISTRIBUTION CODE

13. ABSTRACT (maximum 200 words)

   The Lineate Image Near Ultraviolet Spectrometer (LINUS) is a spectral imager developed to operate in the 0.3-0.4 micron spectral region. The 2-D imager operates with a scan mirror, forming image scenes over time intervals of 10-20 minutes. Sensor calibration was conducted in the laboratory, and the system response to Sulfur Dioxide (SO_2) gas was determined. The absorption profile for SO_2 was measured, and curves of growth were constructed as a function of gas concentration. Test measurements were performed at the Naval Postgraduate School (NPS), from the roof of Spanagel Hall. Field observations were conducted at a coal-burning factory site at Concord, CA with the purpose of quantifying the presence of SO_2. The Concord field measurement showed traces of SO_2, with further analysis still required.

14. SUBJECT TERMS Sulfur Dioxide (SO_2), Remote Sensing, Ultraviolet (UV) Spectral Imaging, LINUS,	15. NUMBER OF PAGES 71
	16. PRICE CODE

17. SECURITY CLASSIFICATION OF REPORT Unclassified	18. SECURITY CLASSIFICATION OF THIS PAGE Unclassified	19. SECURITY CLASSIFICATION OF ABSTRACT Unclassified	20. LIMITATION OF ABSTRACT UL

NSN 7540-01-280-5500

Standard Form 298 (Rev. 2-89)
Prescribed by ANSI Std. 239-18

THIS PAGE INTENTIONALLY LEFT BLANK

REMOTE SENSING OF SULFUR DIOXIDE (SO$_2$) USING THE LINEATE
IMAGING NEAR-ULTRAVIOLET SPECTROMETER (LINUS)

Sing Soong Khoo
Civilian, DSO National Laboratories, Singapore
B.Eng., National University of Singapore, 1995

Submitted in partial fulfillment of the
requirements for the degree of

MASTER OF SCIENCE IN SYSTEMS ENGINEERING (EW)

from the

NAVAL POSTGRADUATE SCHOOL
March 2005

Author: Sing Soong Khoo

Approved by: Richard M. Harkins
                   Thesis Advisor

                   Richard C. Olsen
                   Co-Advisor

                   Dan Boger
                   Chairman, Department of Information Sciences

THIS PAGE INTENTIONALLY LEFT BLANK

ABSTRACT

The Lineate Image Near Ultraviolet Spectrometer (LINUS) is a spectral imager developed to operate in the 0.3-0.4 micron spectral region. The 2-D imager operates with a scan mirror, forming image scenes over time intervals of 10-20 minutes. Sensor calibration was conducted in the laboratory, and the system response to Sulfur Dioxide (SO_2) gas was determined. The absorption profile for SO_2 was measured, and curves of growth were constructed as a function of gas concentration. Test measurements were performed at the Naval Postgraduate School (NPS), from the roof of Spanagel Hall. Field observations were conducted at a coal-burning factory site at Concord, CA with the purpose of quantifying the presence of SO_2. The Concord field measurement showed traces of SO_2, with further analysis still required.

THIS PAGE INTENTIONALLY LEFT BLANK

TABLE OF CONTENTS

LIST OF FIGURES

THIS PAGE INTENTIONALLY LEFT BLANK

LIST OF TABLES

THIS PAGE INTENTIONALLY LEFT BLANK

ACKNOWLEDGMENTS

THIS PAGE INTENTIONALLY LEFT BLANK

I.   INTRODUCTION

A.   PROJECT CONTEXT

This thesis explores the utility of spectral imagery in the near-ultraviolet portion of the electromagnetic spectrum. The spectral region from 0.3-0.4 microns is, in general, poorly exploited in remote sensing, and the work described here is part of a nearly unique study effort in this spectral regime. The work described here deals with the development and use of the Lineate Near Ultraviolet Spectrometer (LINUS). LINUS was designed and built at the Naval Postgraduate School by Professor D. Scott Davis. Initial tests of the sensor in the field in 2002 revealed a variety of problems with the instrument, and subsequent work in the last 2 years has focused on addressing these. In particular, Rodrigo Cabezas added a bore-sighted visual camera and modified the control software to handle new hardware (Cabezas [4]). Significant changes were made in the external hardware (computer, controllers). As the next step in the development of LINUS, significant laboratory experimentation (calibration) and field data collection work have been done, as described here.

B.   PROJECT OBJECTIVE

The objectives of this thesis research were to :

(i)   Conduct laboratory calibrations of the instrument, particularly for the SO_2 response of the sensor. This includes the calculation of the curve of growth.

(ii)   Deploy and test LINUS in the field by observing SO_2 emission data from coal-burning plants.

These objectives were designed to assess the system integration and determine the operational capability of LINUS.   Both objectives were accomplished in this thesis.

C.   OUTLINE

The thesis is written in six chapters and two appendices. Following this Introduction Chapter, Chapter II gives a general description on the operation of LINUS. Chapter III introduces the topic on Natural Sources of Sulfur Dioxide (SO_2) which is the trace gas used in this research. Chapter IV illustrates the experimentation setup and results conducted in the laboratory. Chapter V gives the details of the field data collection made and its data analysis. The last chapter is the conclusion and recommendations. The experimentation procedures and other useful information are placed in the appendices for future reference.

II. GENERAL OPERATIONS OF LINUS

A. PURPOSE

The purpose of this chapter is to introduce LINUS to the reader by presenting a brief description of its design, operation and control. More detailed information can be obtained by referring to completed theses on this topic by Kompatzki, 2000 [1], Gray, 2002 [2], Halvatzis, 2002 [3] and Cabezas, 2004 [4].

B. LINUS AS AN IMAGING SPECTROMETER

As the name suggested, LINUS can function as an imager and also a spectrometer in the UV spectrum. An imager can form a two dimensional (2-D) image of the captured scene and present the spatial characteristic to the observer. The observer is then able to discriminate, detect, identify, classify and associate, and recognize the target(s). General features and patterns like size, shape and color are used for spatial discrimination. By capturing a series a real-time imagery, temporal algorithms can also be used for target detection. However, when the target is heavily camouflaged, by blending its surface colors into its surroundings, like a chameleon or an octopus, or when the target versus background contrast is poor, the target detection capability of the imager will be limited or reduced. This limitation can be corrected by looking at various spectrums to eliminate the dependence on a fixed waveband used in an imager.

A spectrometer is able to separate the received irradiance into its contributing spectral content as a function of wavelength (λ) or frequency (f). By studying and identifying the spectral characteristics of different materials, this important information can be used in target detection. For example, the red and blue "spikes" can be observed from a mid-infrared spectral plot of an aircraft exhaust or a missile plume. Although spectroscopy is a robust technique, it is also very time consuming because it can take a long time to complete the data collection. Typically, the time needed for the spectrometer to complete one full spectrum, is in the order of seconds. The imager is much faster by working at a

typical frame rate of 30Hz or a frame time of 33 msec. The primary purpose of LINUS, a spectrometer, is enhanced with the addition of a scanning mirror to cover the azimuth angle to produce an image of the scene. More details will be given in the next section.

C.   DESIGN AND CONFIGURATION

1.   Diffraction Grating

LINUS optical design uses a diffraction grating to produce the spectrum display. The diffraction grating disperses the incident radiation into its higher order spatial frequency components. Its fundamental frequency is equal to the inverse of the slit spacing. .

The diffraction optics can be simply put as an N large number of very fine saw-tooth gratings that are equally spaced. These small saw-tooth gratings will disperse the incident light source into its spectral line components. The resulting interference (diffraction) pattern shows an irradiance distribution function at the image plane governed by the following equations from Pedrotti [5]:

$$I(\theta) = I_0 \left(\frac{\sin \beta}{\beta} \right)^2 \left(\frac{\sin N\alpha}{\sin \alpha} \right)^2 \tag{1}$$

where, I_0 is the peak irradiance at $\theta = 0$

$\beta = \frac{1}{2} k b \sin\theta$,   b is the slit width

$\alpha = \frac{1}{2} k a \sin\theta$,   a is the slit spacing

$k = \frac{2\pi}{\lambda}$ and θ is the angle of the diffraction

The grating equation works out to be:

$$a \sin \theta_m = m\lambda, \tag{2}$$

where,   m = 0, ±1, ±2,… (in general) is known as the diffraction order

θ_m is the diffracted light angle where the maxima occurs

For LINUS, the diffraction order is set to 1 to reduce complications due to overlapping orders. In other words, for each different wavelength λ_i, the maxima will be uniquely diffracted to an incident angle, θ_i, which corresponds to a position x_i on the focal plane array. The limit of resolution for this system is given by: $\Delta\lambda_{min} = \lambda / N$, for the 1st diffraction order derived from Pedrotti [5] with resolving power $\mathfrak{R} = m*N$ and set m= 1.

"The diffraction grating used in LINUS is a 2 inches square with 600 groves per millimeter" from Gray [2]. This gives N = 2*25.4*600 = 30480. At λ = 300 nm, $\Delta\lambda_{min} \approx 0.01$ nm theoretically. In practice, "the grating is orientated to span wavelengths from 282.4 to 316.9 nm", Gray [2]. Based on the CCD detector size and the focal length, the spectral resolution is computed to be (316.9 − 282.4)/512 $\approx$ 0.07 nm. Comparing with $\Delta\lambda_{min}$., approximately 7 maximas will be integrated in each detector pixel.

2. LINUS Optical Design

LINUS is designed for remote sensing measurements of atmospheric gas plumes. It works primarily in the UVB waveband (280 - 320 nm) where the solar radiation is able to penetrate through the ozone layer, in the stratosphere and illuminate the environment. Solar radiation is fully absorbed for the UVC waveband (200 – 280 nm), also known as the solar-blind region. LINUS gas detection is based on the spectral absorption of photons by the gas molecules mainly due to electrons transition from lower states to higher states in discrete levels using Rayleigh scattering of the aerosol and gas molecules as the illumination source. For this thesis, Sulfur Dioxide (SO_2) is chosen as the trace atmospheric gas for study and evaluation. It has a strong absorption band around 300 nm in the working UVB waveband for LINUS, and is also a primary pollutant emitted from volcanic plumes and industrial smokestacks.

The schematic block diagram for LINUS design is shown in Figure 1. It shows the fundamental components that make up the instrument. The optical path is denoted by the block arrow and the electrical signal is denoted by the blue arrow line. The Host Control Module contains the software and hardware to 1) control the movement of the scanning mirror, 2) capture the visual and UV images, and 3) present the UV camera controls to the user.

The detailed optical layout is modified from Davis [6] and shown in Figure 2. This diagram shows the path of the input radiation to the cameras and the individual optical components inside the black box of LINUS as depicted in Figure 3. As seen from the tracing of the incoming rays, the far field radiation (also known as Fraunhofer Region) first encounters a scanning mirror (for subsequent purpose of image scanning) which then reflects into a bandpass filter and a telescopic assembly consisting of a primary focusing objective and a collimator lens. A thin variable slit is in between the two telescopic lenses to control the exposure strength and spectrum resolution. The output of the telescopic lens is a collimated beam that hits the reflection grating and disperses into their line spectra (quite similar to the dispersion in a prism but different in principle). The dispersed rays are collected by the camera objective and focused

at the UV intensified camera. Included in the optical layout, is a visual camera added by Cabezas [4] for the purpose of visual aiming and comparison with the final UV output scene. The scanning mirror rotates to the proper alignment position to reflect the input radiation into the visual camera instead of the collection optics for the UV camera. This routine is commanded automatically using the Labview program. The design configuration for the visual camera was chosen for its simplicity and minimal impact to the original layout by Davis [6]. The only limitation is that it does not allow for viewing of both cameras at the same time. This is not a major issue since LINUS is not suited for real-time applications.
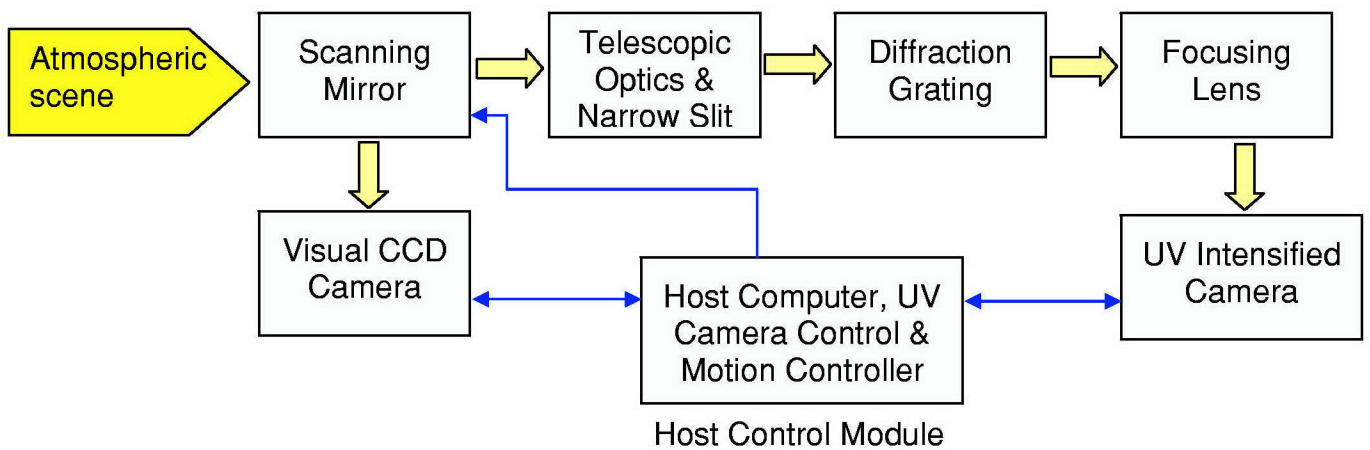
Figure 1.   Schematic Block Diagram for LINUS
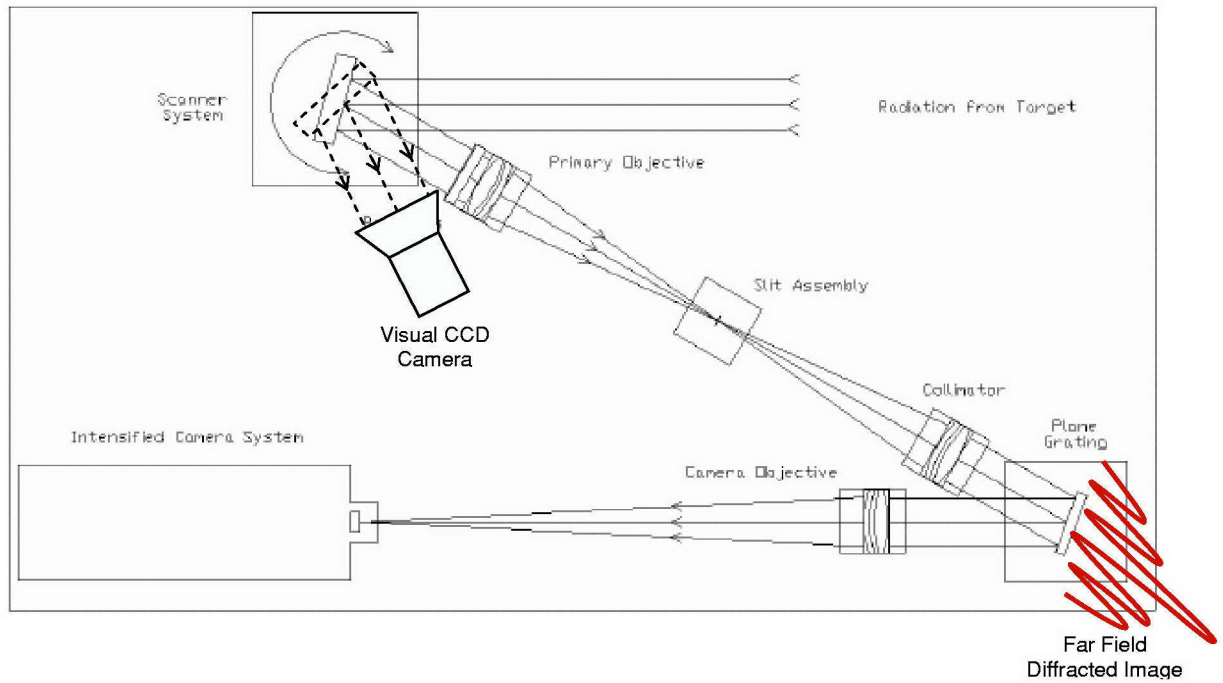
Figure 2.   Optical Layout of LINUS (After Davis [6])
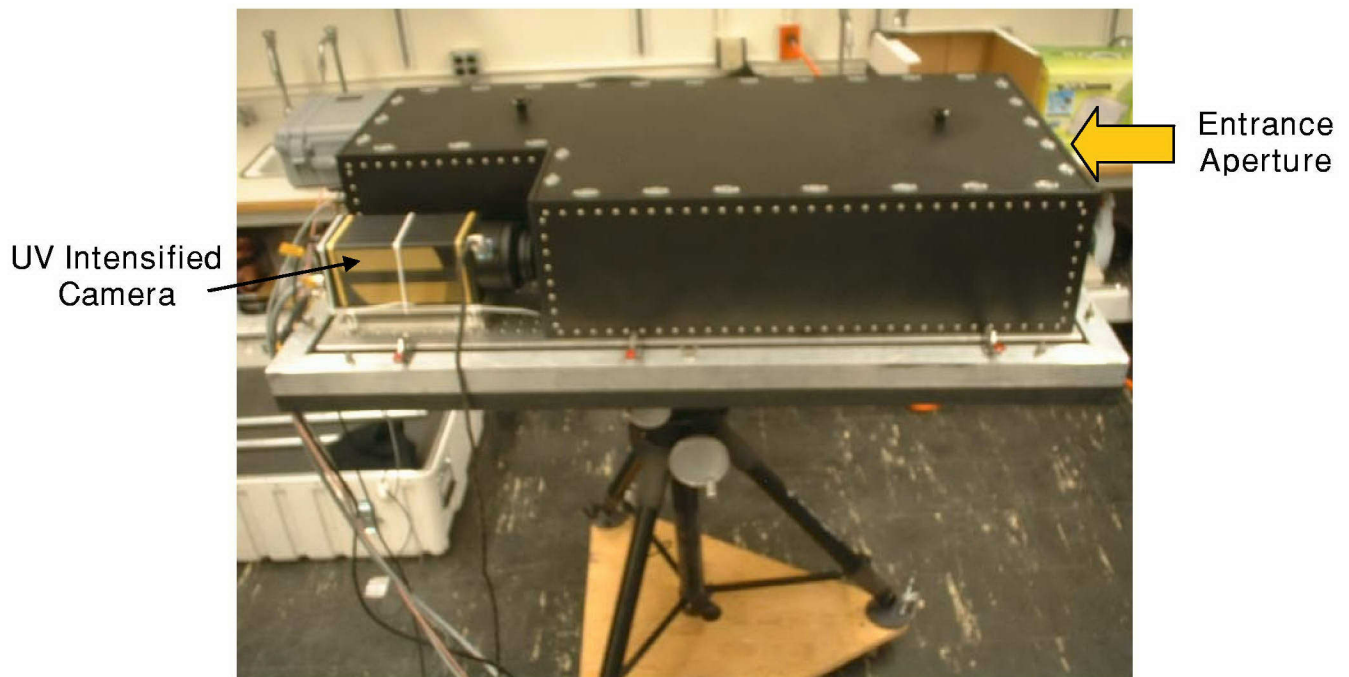
Figure 3.   LINUS Optical System

At each frame, a narrow vertical strip of pixels is transformed into a two dimension (2-D) spectral image of 512 x 512 pixels as shown in Figure 4. The horizontal axis on the UV camera corresponds to a set of wavelengths and the vertical axis corresponds to the equivalent vertical spatial coordinates of the image scene. Each pixel on the narrow vertical strip is dispersed by the diffraction grating into a row of its spectral components and then focused onto the focal plane array. The scanning mirror then steps through the scene in small increments, to image adjacent vertical strips until the entire scene is covered. By appending individual, consecutive, spectral frames, a hyperspectral cube is built consisting of the vertical and horizontal spatial characteristics. This produces the spectrum of the spatial coordinates in the FOV. The data cube is shown in Figure 5. Post-analysis of the data cube using ENVI or IDL allows the reconstruction of the 2-D field of view of the UV scene which can be compared with the stored visual image.
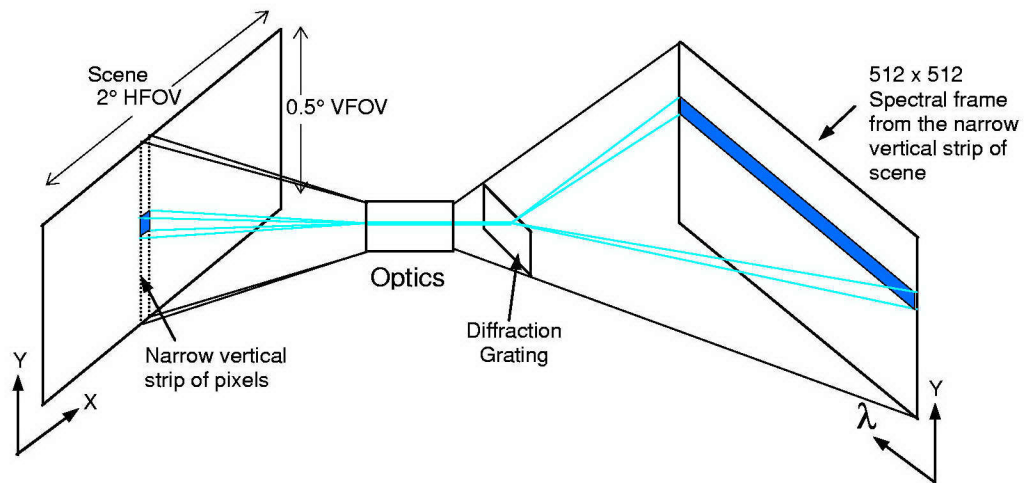
Figure 4.   LINUS Spectral Acquisition Schematic Diagram
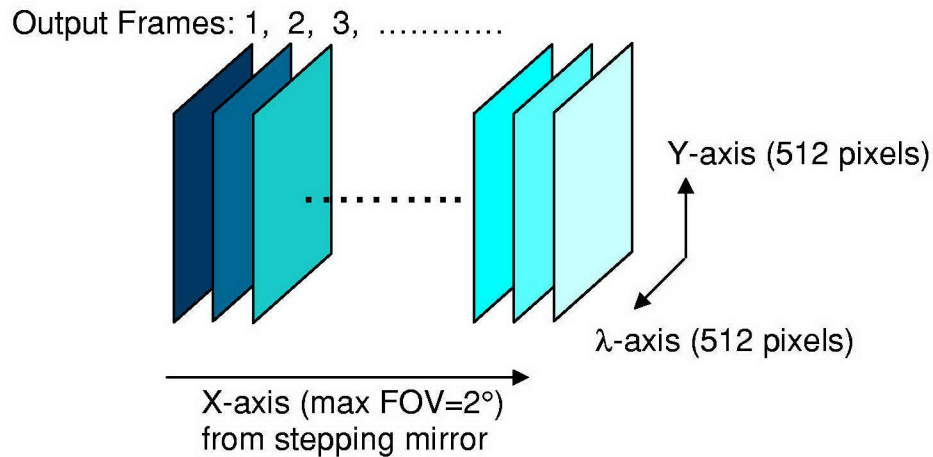
Figure 5.   Hyper Spectral Data Cube Formed by LINUS Output

D.   SOFTWARE CONTROL AND OPERATION

1.   Software

Other than the optical system, LINUS also has a Host Control Module to operate the scanning mirror and the acquisition, storage and processing of the camera images. The Host Control Module is pictured in Figure 6, all packed into a field deployable storage case, which consists of a host computer, the UV camera temperature controller, the UV camera pulse generator and the motion controller with its power amplifier.

The operation of LINUS is automated using the LabView program. The program automates the motion of the scanning mirror, the settings of the UV camera and the image acquisition of the visual and UV cameras. A sample of the control window is shown in Figure 7. The start up and shut down procedure can be found in Appendix A. Also given, is a quick guide on the operation of this program for new user to learn to operate LINUS quickly.
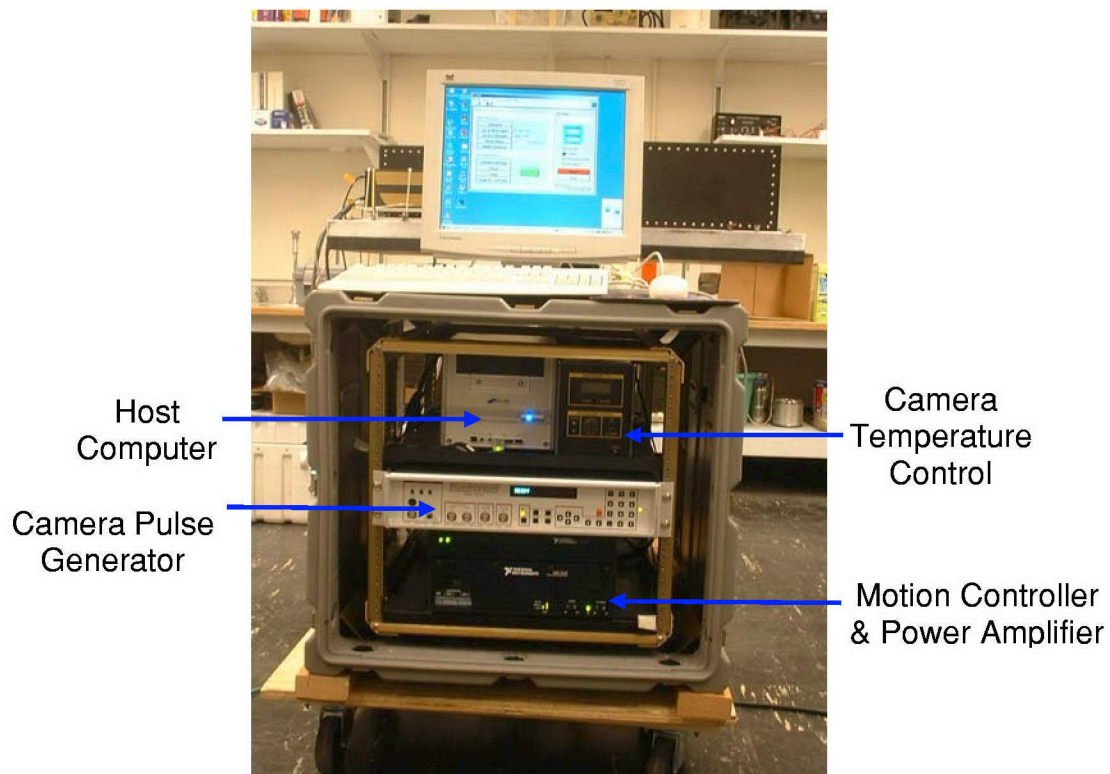
Figure 6.   Host Control Module for LINUS
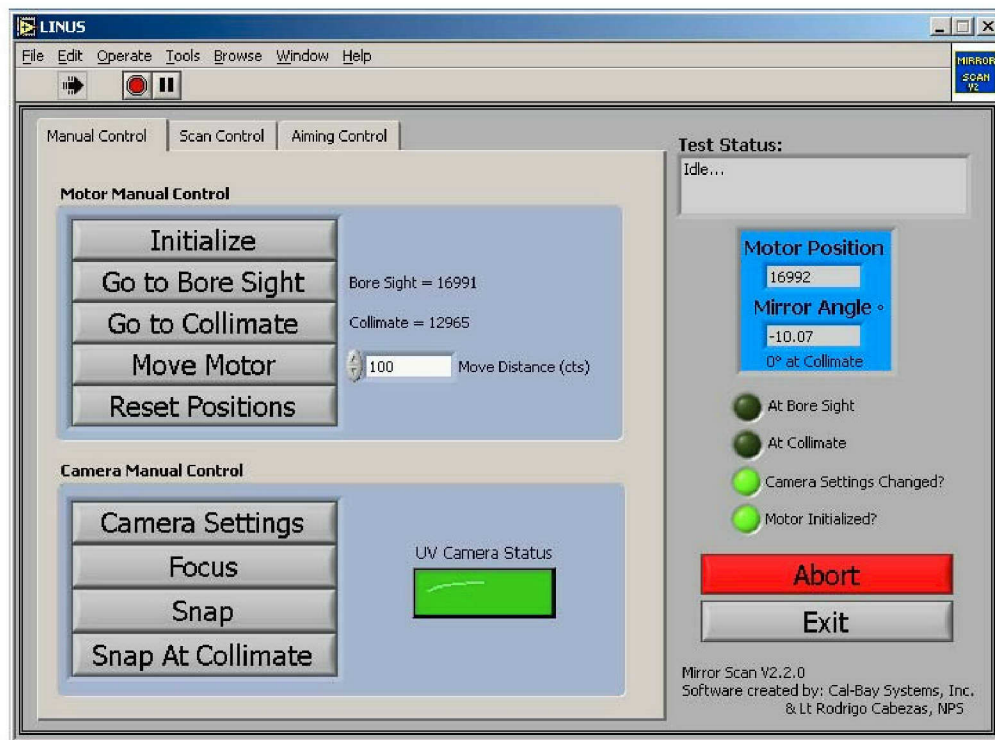
Figure 7.   LabView Software Control Panel

2.   Wavelength Calibration

As the scene of a narrow vertical slit is diffracted and imaged onto a 512 x 512 focal plane array, the wavelength information is embedded in the pixel number for the horizontal axis of the detector array. The pixel number has to be calibrated to its corresponding wavelength in order to analyze the spectrum. The latest calibration was performed by Cabezas [4] using a hollow cathode platinum lamp as the illumination source. The platinum (Pt) lamp was selected for its known characteristic spectral emission in UVB waveband. By matching the measured peaks for the Pt lamp against NIST standard data, Cabezas [4] gave the calibration equation to be:

$$\text{Wavelength} = 2776.58 + 0.8299 * \text{Pixel Number} \qquad (3)$$

This calibration equation is needed in the analysis of the laboratory experiment and field data measurements. However, one has to be careful when using the calibration Equation (3), to ensure that the pixel number is in the correct order. When the spectral data is collected and stored, the pixel number actually corresponds to a reverse order for the wavelength, i.e., the data corresponds to a descending wavelength instead of ascending as given by Equation (3). In the post-processing of the data cube, a "REVERSE" function in IDL is called to correct the sequence order to match Equation (3).

III.   NATURAL SOURCES OF SULFUR DIOXIDE (SO_2)

A.   PURPOSE

This chapter provides a brief understanding on the characteristics of the trace gas SO_2 and focuses at the natural sources produced by volcanic eruption.

B.   CHARACTERISTICS OF SULFUR DIOXDE (SO_2)

Sulfur dioxide (SO_2) is a colorless gas with a sharp, irritating odor that makes one choke when inhaled. It is produced from the burning of fossil fuels (coal and oil) and the smelting of mineral ores that contain the sulfur species in the form of sulfates and sulfides. Natural sources of sulfur dioxide include releases from volcanoes, oceans, biological decay and forest fires, of which erupting volcanoes account for a significant amount of SO_2 emissions. Volcanoes contribute ~50% of the SO_2 in the Earth's atmosphere.

SO_2 is a major pollutant to the Earth's atmosphere and affects human health when excessively inhaled, It creates acid rain that destroys buildings and metal structures, and damages the ozone layer that protects us from the harmful UV radiation. It is important to study SO_2 for public health and environmental concerns.

C. SO_2 FROM VOLCANIC ERUPTION

Volcanic eruption involves the movement of the magma from underneath to the surface of the Earth. Magma refers to the molten substance consisting of a complex mixture of silicate liquid and solid crystals and a range of dissolved gases called volatiles. The volatiles include water (H_2O), carbon dioxide (CO_2), sulfur dioxide (SO_2) as the dominant abundant, and other halogens (Fluorine, Chlorine) and noble gases (He, Ar, B) in lesser abundance. These volatiles are dissolved in the silicate melted portion of the magma, at high pressure, when underneath the earth. As the magma ascends towards the Earth's surface, the pressure is decreased as well as the solubility of the volatiles. This causes the

13

volatiles to form back into their gaseous state. The result is a tremendous expansion force which creates a volcanic eruption as shown in Figure 8. A simple analogy to this is the popping of a champagne bottle cork when shaken vigorously to generate the air bubble volume inside. Scientists regularly measure the level of SO_2 surrounding a volcano for indication of an impending eruption when there is sign of rapid increase.

Volcanic gases are typically released from an active crater through its exhaust cracks and vents. Some low-temperature gases can also diffuse through a volcano's porous flanks to the surface which are a some distance away from the active crater area. Even for a sleeping volcano like the Lassen Volcanic National Park, there is constantly an on-going degassing process through the soil and springs several kilometers away. Scientists suspect that the diffuse flank, degassing through faults and fractures, can play an important role in channeling the gases to the surface and reduce the build-up for a volcanic eruption.

The sulfur species exists in volcanic gases are mainly composed of SO_2 and H_2S and they are closely related in chemical equilibrium for different temperature and pressure conditions by the reaction Equation (4) (from ."Encyclopedia of Volcanoes" [8])

$$SO_2 + 3H_2 \Leftrightarrow H_2S + 2H_2O \qquad (4)$$

This equation is important as it involves the major gas species in the volatiles. Studies showed that the reaction would favor the predominant of H_2S and H_2O species at high pressures when the magma degasses at greater depth. Similarly, H_2S is dominant over SO_2 when the volcanic gases are cooled.

During the degassing process, it is possible for the rising gases to encounter hydrothermal water, ground water or shallow reservoirs. SO_2 is readily soluble with H_2O and reacts to produce sulfuric acid (H_2SO_4). In some instance, it also reacts to give elemental sulfur (S) as found in hot spring. *"Interaction of hot magmatic gases with shallow ground water or a hydrothermal system results in a volcanic gas discharge characterized by ... low SO_2/H_2S ratio."* ((from

14

."Encyclopedia of Volcanoes" page 809 [8]). In conclusion, the SO_2 abundance level may not be high near volcanic parks.

maximum plume height

H_t

spreading of plume as a gravity current

Umbrella region

H_b
level of neutral buoyancy

Convective phase
(plume rises by buoyant convection)

plume density<atmosphere

Pumice and ash fallout

Jet phase
(motion dominated by initial vertical momentum)

jet density>atmosphere

Source mixture of hot pyroclasts and gas

Conduit

Fragmentation region

Steady supply of magma from the chamber

Magma with exsolved volatiles

Exsolution surface

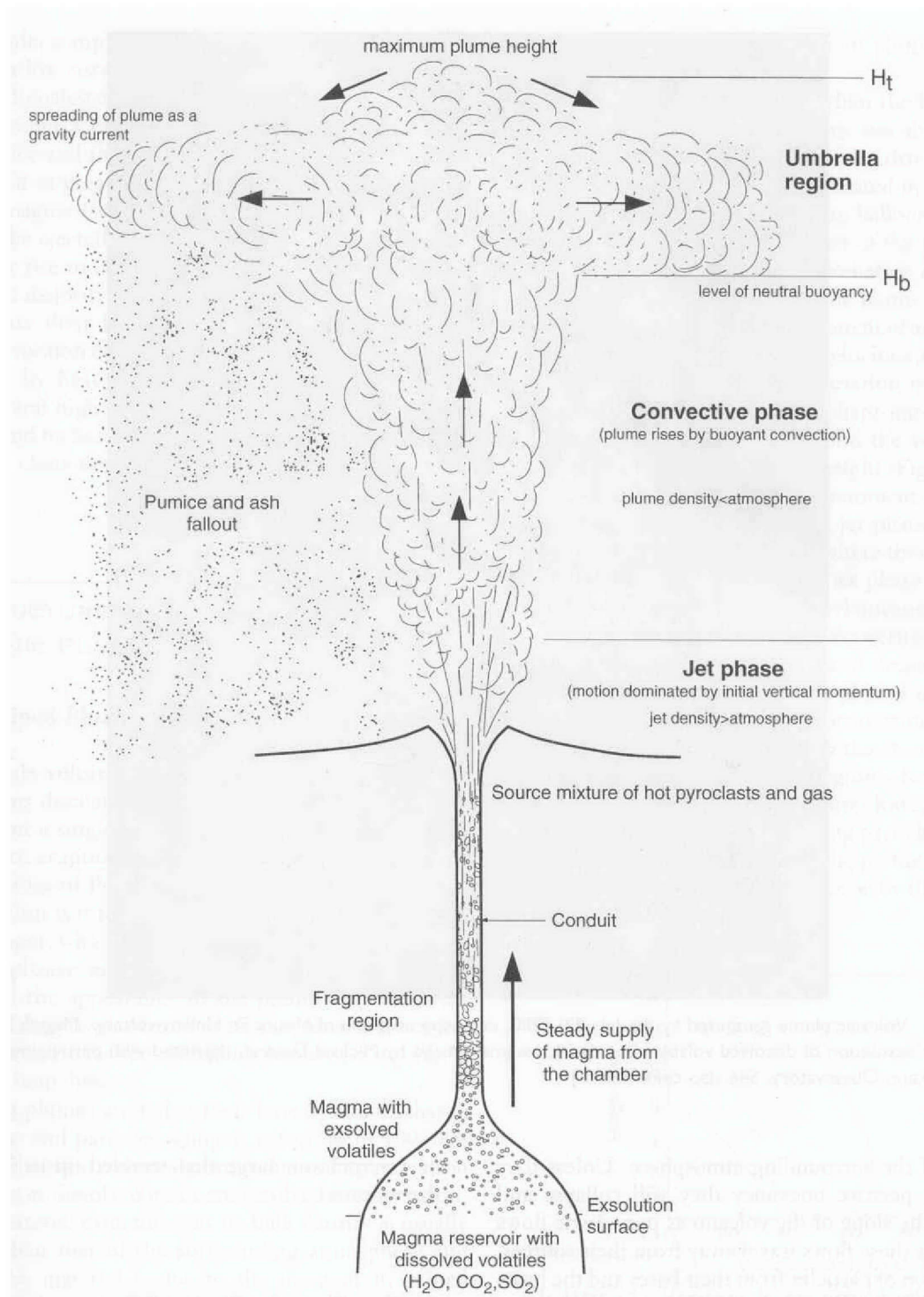Magma reservoir with dissolved volatiles (H_2O, CO_2, SO_2)

Figure 8.   Formation of a Volcanic Plume by Degassing of Volatiles (H_2O, CO_2 and SO_2) from a High Silica Magma (From "Encyclopedia of Volcanoes" [8])

THIS PAGE INTENTIONALLY LEFT BLANK

IV. LABORATORY MEASUREMENT AND CALIBRATION

A. PURPOSE

The purpose of this chapter is to discuss the partial pressure measurement and determine the curve of growth for the Sulfur Dioxide (SO_2) gas in the laboratory before bringing out LINUS for field data collection.

B. EXPERIMENT SETUP AND ALIGNMENT

The setup for the laboratory experiment requires careful alignment in order to ensure consistency and accurate measurement. The schematic diagram of the experiment setup is shown in Figure 9. The alignment requires LINUS to be pointed into the center of the test cell and at the collimating mirror to receive the radiation of the deuterium lamp. Since LINUS is big and bulky, it can be quite tedious to get the alignment right with its narrow FOV. With a slit width of 0.11mm, the instantaneous FOV is 0.025° x 0.5°. The Helium Neon (HeNe) laser, with two opposite sided beams, is used for alignment. The setup is shown in Figure 10. The HeNe laser is placed at the center of the optical path between the collimating mirror and the test cell. First, the operator aligns the laser with its output facing the mirror to be spotted on the deuterium lamp. The LINUS scanning mirror is set at the bore-sight position. Then the laser spot is set near the center of the entrance aperture and the tripod knobs are adjusted so that the returned laser beam lands back onto the laser. The laser is then removed, and the visual camera is enabled in the camera control program to verify that the alignment is accurate by using the marked crosshair as a reference. At this point, the scan mirror is set to collimate position for the UV camera and view using the focus mode. Fine adjustments can now be made by tuning the collimating mirror to give the strongest UV signal measured by LINUS and to position the spectrum at the center of the screen. The alignment procedure is then completed.
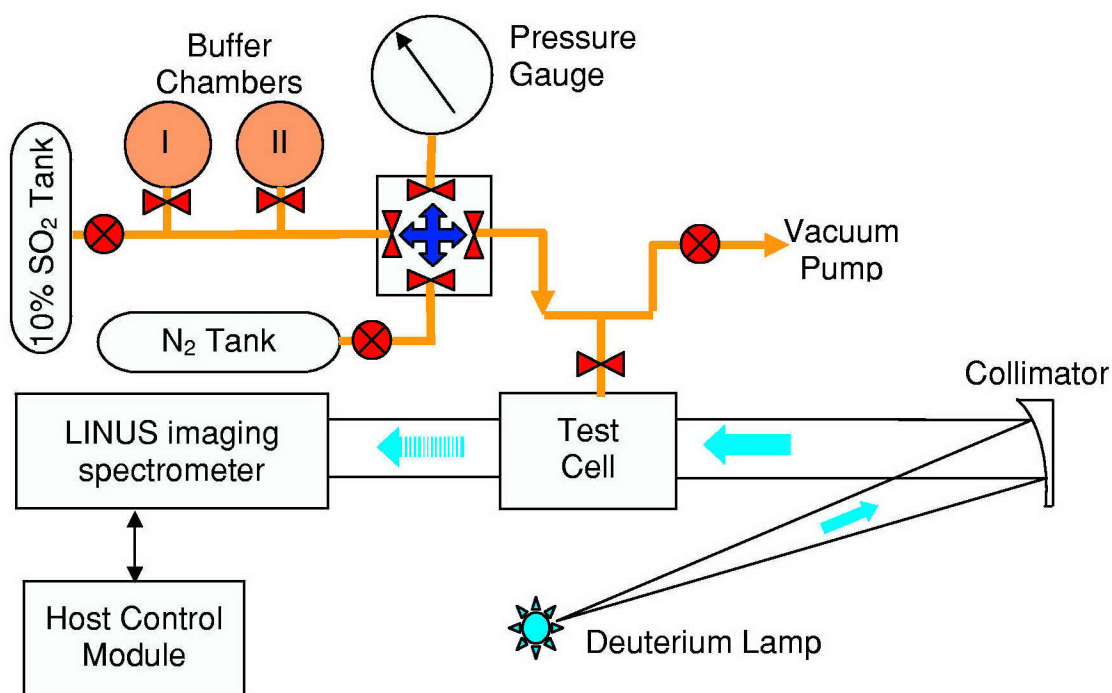
Figure 9.   Experiment Setup for Partial Pressure Measurement
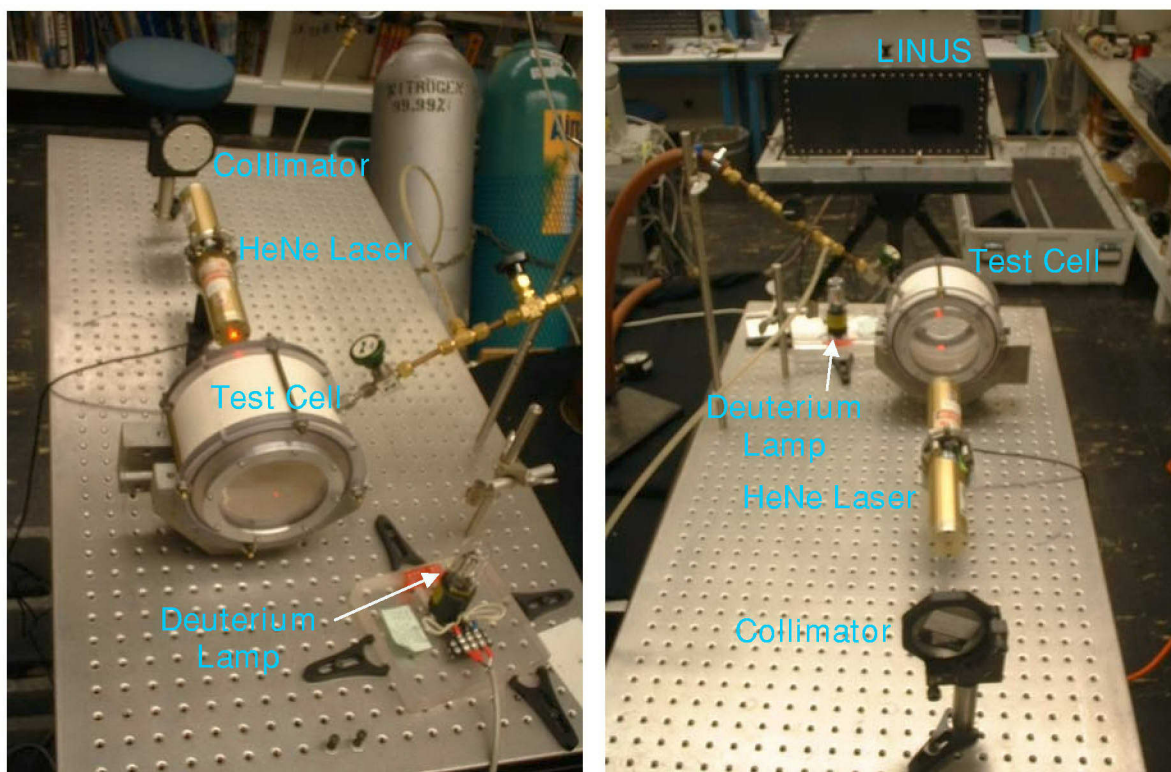
Figure 10.   Alignment for the Experiment Setup

C.   PARTIAL PRESSURE MEASUREMENT

    1.   Laboratory Data Collection

    The procedure used to conduct the partial pressure measurement is given in Appendix B using the setup shown in Figure 9. Two mixing or buffer chambers of similar volume are used to dilute the SO_2 concentration with high purity Nitrogen (N_2). If the small volume of tubing is ignored, the concentration of the SO_2 will be halved for each mixing cycle. However, it is found that the concentration is reduced proportionally by 0.4657 instead of 0.5 for each mixing due to the tubing. This procedure allows more data sets to be collected as compared to the work done by Gray [2] and Marino [7].

    The gas test cell used for this experiment is the small quartz test cell that measures 4 inches in diameter and 3.25 cm for the inner path length. A wideband UV source is needed as the reference source to determine the absorption of SO_2 for each partial pressure and concentration. The deuterium lamp is used as the illumination source. By taking the ratio of the UV signal measured with the test cell filled with SO_2 and at vacuum, the SO_2 absorption profile can be determined for different pressure and concentration to determine the curve of growth.

    The LINUS parameters used for the partial pressure measurement are given in Table 1. The Focus mode is used to adjust the integration time and MCP voltage such that the spectral image is not saturated with the measured signal at full range to be around 2000 DN (digital number). This number is a relative pixel intensity based on how many bits are used for the A/D (analog to digital) conversion. The A/D range is from 0 to 4095 for the UV camera. A high value of more than 4000 DN is deemed as saturated.

19

Table 1.   LINUS Parameters for SO_2 Partial Pressure Measurement

Slit Width	0.11 mm
Integration Time	2 sec
MCP Voltage	710 V
Start Absolute	12990
Counts/Step	5
Steps	10

Table 2.   Data Collected for Different SO_2 Pressure and Concentration

Concentration of SO_2	Partial Pressure (Torr/mm Hg)
10%	185, 275, 365, 450, 550, 640
4.66%	185, 275, 365, 450, 550, 640
2.17%	185, 275, 365, 450, 550, 640
1.01%	185, 275, 365, 450, 550, 640
0.47%	275, 365, 450, 550, 640
0.22%	550, 640

2.   Data Analysis

For each SO₂ setting, one vacuum measurement is made before the test cell is filled with SO₂ with a specific pressure and concentration. This is to minimize the error due to the variation of intensity of the deuterium lamp output. Ten image frames that span across the collimated center at 5 increment counts are captured for each data set to average out and reduce the error due to noise. Each measured data set is stored as a 3-D matrix of size [512,512,10]. An IDL program "SO2_CAL" is compiled to extract, process and view the result of the data sets. For one who is less familiar with the function call for IDL but more familiar with the toolbox for Excel, the processed data is exported using the "WRITE_SYLK" command in IDL to Excel files for further manipulation and graph plotting. The results for SO₂ absorption profiles are shown in Figure 11.

Four specific lines of absorption are identified which corresponds to Pixel Row # 200 (wavelength 2943 Å), Pixel Row # 228 (wavelength 2966 Å), Pixel Row # 256 (wavelength 2989 Å) and Pixel Row # 283 (wavelength 3012 Å). These four absorption lines are selected as they are near to the center of the bandpass filter (@ 2984 Å) to give maximum response. The SO₂ transmission values at these four absorption lines are extracted for analysis. The absorption of SO₂ for different partial pressure and concentration are correlated by computing the SO₂ column abundance (#molecules/m²) for the parameters in Table 2 using Equation (5). The extracted transmission values are tagged to the computed column abundance and sorted in ascending order manner. The result is shown in Table 3 and plotted in Figure 12. The Lorentz model is found to be a good fit to the plots of Figure 12 using the software tools from Origin® 6.1.

$$n(molecules/m^{-2}) = \frac{P(torr)*133.32}{R*T} * 6.022 x 10^{23} * Depth * Conc(SO_2) \quad (5)$$

$$R(J.k.mol^{-1}) = 8.31441$$

Where, $T(K) = T(°C) + 273.15 = 294.55K$ (room temperature)
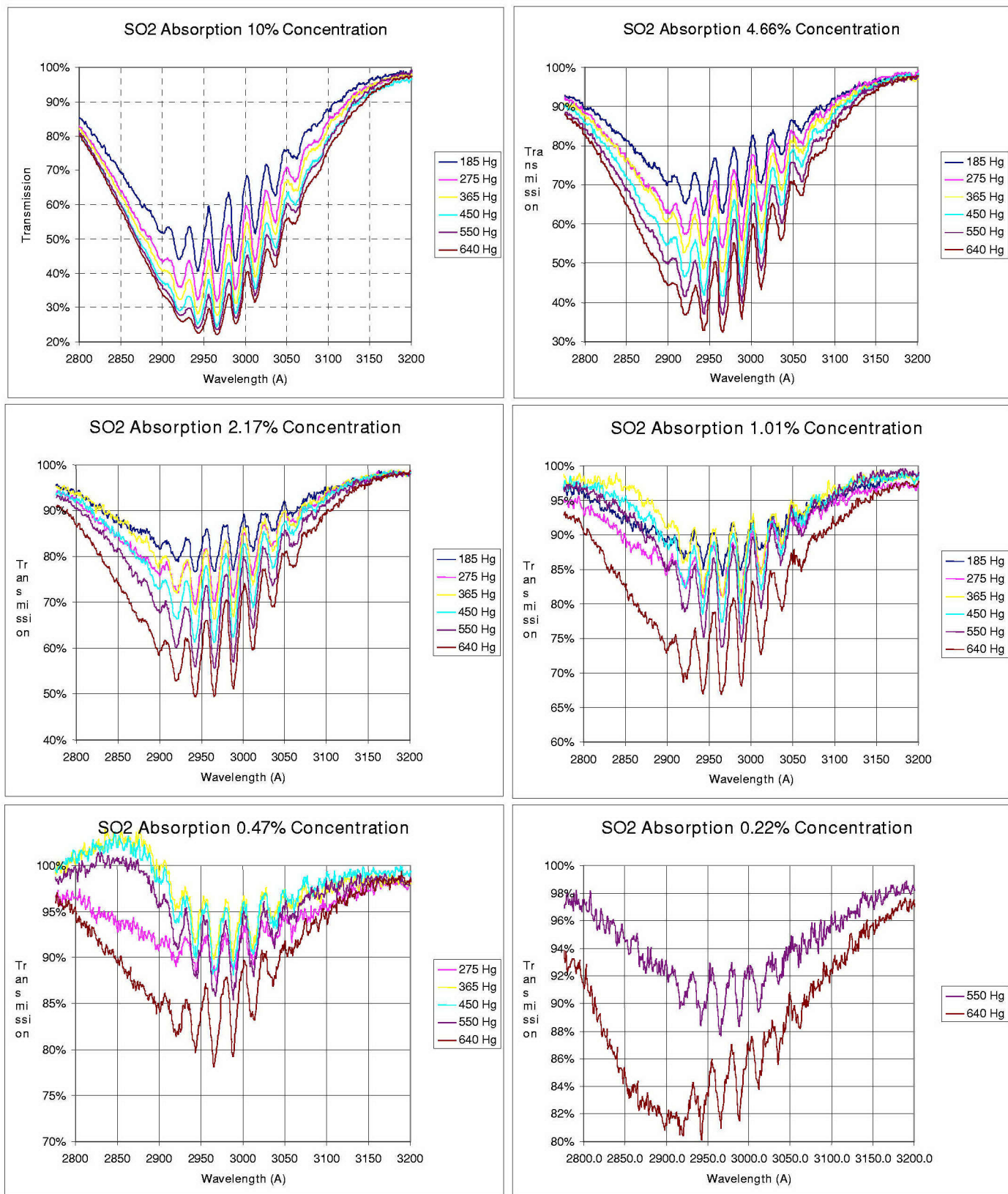
$$Depth = 0.0325m$$

Figure 11. Results for SO_2 Absorption for Different Pressure and Concentration
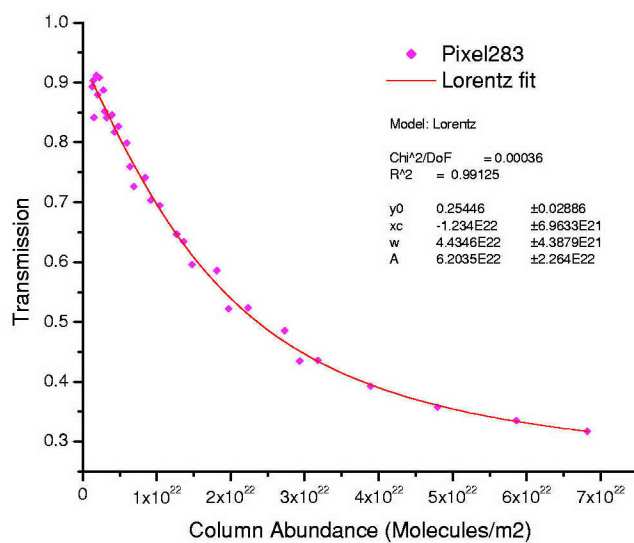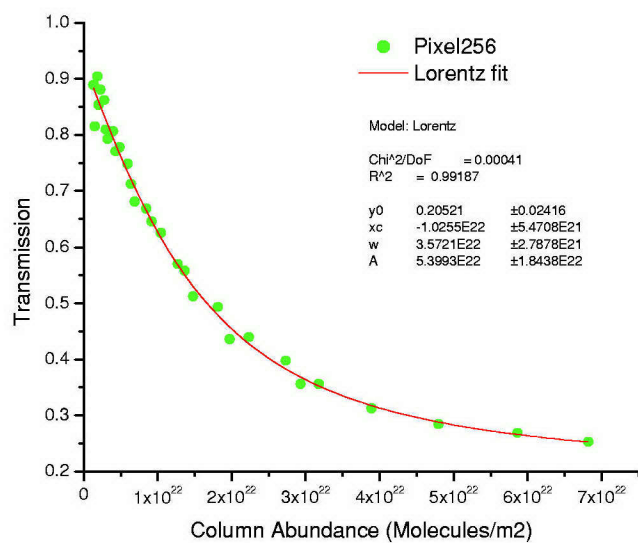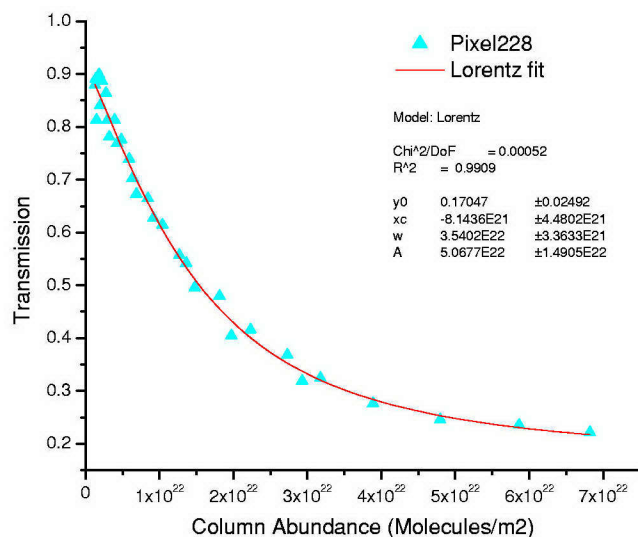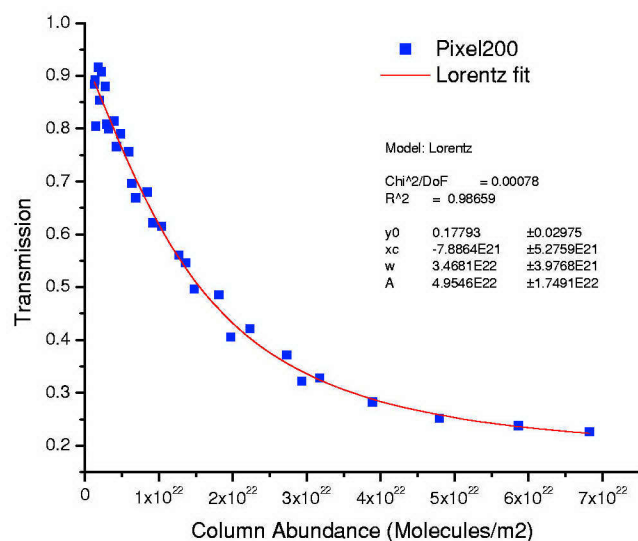
Figure 12. Transmission Loss Due to SO_2 Absorption at Wavelength = 2943Å, 2966Å, 2989Å & 3012Å

Table 3.   Percentage of Transmission Loss Due to Presence of SO$_2$

Pressure	Concentration	Molecules/m^2	Pixel 200 or $\lambda = 2943$Å	Pixel 228 or $\lambda = 2966$Å	Pixel 256 or $\lambda = 2989$Å	Pixel 283 or $\lambda = 3012$Å
550	0.22%	1.284E+21	88.42%	87.92%	88.92%	89.36%
275	0.47%	1.378E+21	89.18%	89.10%	88.85%	90.31%
640	0.22%	1.494E+21	80.50%	81.29%	81.49%	84.17%
365	0.47%	1.829E+21	91.65%	89.90%	90.40%	91.18%
185	1.01%	1.991E+21	85.42%	84.04%	85.34%	87.91%
450	0.47%	2.255E+21	90.78%	88.67%	88.10%	90.81%
550	0.47%	2.756E+21	87.98%	86.37%	86.21%	88.76%
275	1.01%	2.959E+21	80.83%	81.24%	80.98%	85.20%
640	0.47%	3.207E+21	79.92%	78.07%	79.27%	84.14%
365	1.01%	3.928E+21	81.41%	81.26%	80.64%	84.53%
185	2.17%	4.275E+21	76.59%	76.85%	77.10%	81.72%
450	1.01%	4.842E+21	79.01%	77.54%	77.84%	82.69%
550	1.01%	5.918E+21	75.61%	73.90%	74.87%	79.89%
275	2.17%	6.354E+21	69.66%	70.29%	71.24%	75.91%
640	1.01%	6.887E+21	66.87%	67.29%	68.12%	72.65%
365	2.17%	8.434E+21	67.99%	66.43%	66.87%	74.08%
185	4.66%	9.179E+21	62.19%	62.73%	64.59%	70.34%
450	2.17%	1.040E+22	61.50%	61.45%	62.54%	69.45%
550	2.17%	1.271E+22	56.06%	55.69%	56.96%	64.65%
275	4.66%	1.364E+22	54.61%	54.17%	55.80%	63.44%
640	2.17%	1.479E+22	49.63%	49.55%	51.23%	59.61%
365	4.66%	1.811E+22	48.53%	47.94%	49.33%	58.59%
185	10.00%	1.971E+22	40.57%	40.48%	43.59%	52.20%
450	4.66%	2.233E+22	42.16%	41.57%	43.95%	52.38%
550	4.66%	2.729E+22	37.15%	36.80%	39.75%	48.53%
275	10.00%	2.930E+22	32.23%	31.86%	35.61%	43.50%
640	4.66%	3.176E+22	32.79%	32.43%	35.62%	43.57%
365	10.00%	3.889E+22	28.23%	27.61%	31.29%	39.27%
450	10.00%	4.794E+22	25.15%	24.53%	28.43%	35.77%
550	10.00%	5.860E+22	23.79%	23.53%	26.88%	33.52%
640	10.00%	6.819E+22	22.62%	22.12%	25.29%	31.72%

3. Curve of Growth Using Equivalent Line Width

The curve of growth is an empirical graph commonly used in absorption spectroscopy as the means to quantify the absorption profile. The curve is plotted by determining the relationship between the equivalent width of the absorption line versus the concentration of the absorbing material. The equivalent line width (W_λ) is defined as shown in Figure 13 with its area from the baseline $I(\lambda) = y_0$ equal to the area (A) under the Gaussian curve. When $y_0 = 1$, the equivalent line width is then equaled to area (A).
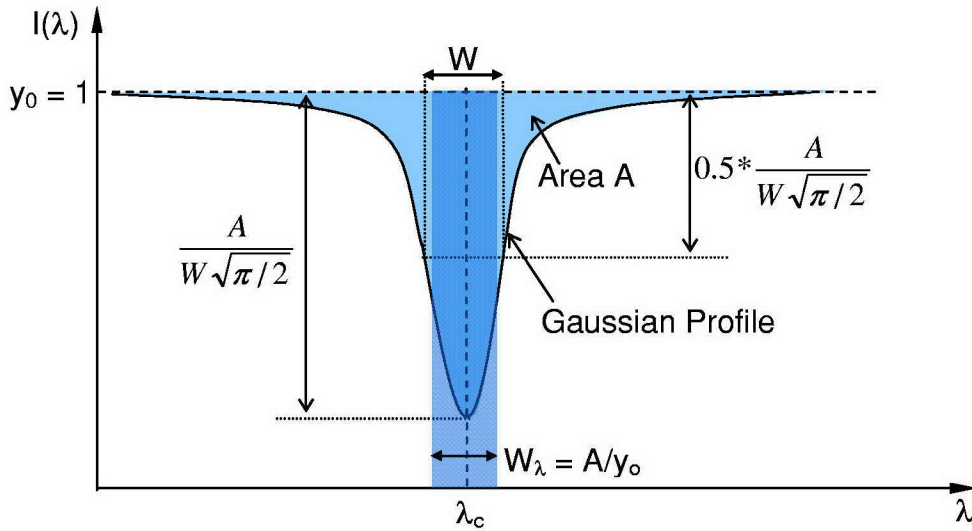
Figure 13. Definition of Equivalent Line Width and Gaussian Parameters

Marino [7] had performed the curve of growth measurement for NUVIS, an earlier version of LINUS and the reader can refer to his thesis for more information. His methodology to compute the line width is adopted here for the full set of data measured using LINUS. The Gaussian line shape, as shown in Figure 13, is used for fitting into the absorption lines formed by SO_2. The equivalent line width is then determined from the parameter "Area" of the Gaussian equation with the parameter $y_0 = 1$. The center of the Gaussian shape is positioned at the SO_2 absorption line for the curve fitting. Instead of using IDL to perform the Gaussian fit as Marino [7] did, Origin® 6.1 is used for its user-

25

friendly tools. The Gaussian equation is also modified as in Equation (6) to accommodate the inverse order of the SO$_2$ absorption profile as shown in Figure 13.

$$f(x) = y_0 - \frac{A}{w*\sqrt{\pi/2}} \exp\left[-2*\left(\frac{x-x_c}{w}\right)^2\right] \tag{6}$$

Where: y_0:   baseline offset = 1 for transmission

A: total area under the Gaussian curve

W: 2σ width of the Gaussian curve at half height

X_c: center of the Gaussian peak

An example of the curve fitting done with its input parameters is shown in Figure 14. For each set of concentration and pressure data set given in Table 2, curve fittings are performed for the absorption lines at 2943Å (Pixel # 200), 2966Å (Pixel # 228), 2898Å (Pixel # 256) and 3011Å (Pixel # 283) as the Gaussian centers (X_c). The fitting ranges for the data sets are given in Table 4. After many rounds of iterations by clicking the "10 Iter." button, the result for the Area (A) and Width (W) of each best fitting is recorded and tabulated in Table 5. The SO$_2$ curve of growth is plotted in Figure 15.

Table 4.   Gaussian Centers and Fitting Range for Origin Curve Fit

Absorption Line (Å)	Pixel #	Fitting Range
2943	200	(192 to 213)
2966	228	(220 to 240)
2898	256	(248 to 267)
3011	283	(274 to 296)

26

Graphical Display for Curve Fitting

Model: GaussFit

Chi^2/DoF = 0.00002
R^2 = 0.97262

y0	1	±0
xc	2989	±0
w	32.26939	±0.6539
A	30.10795	±0.5593
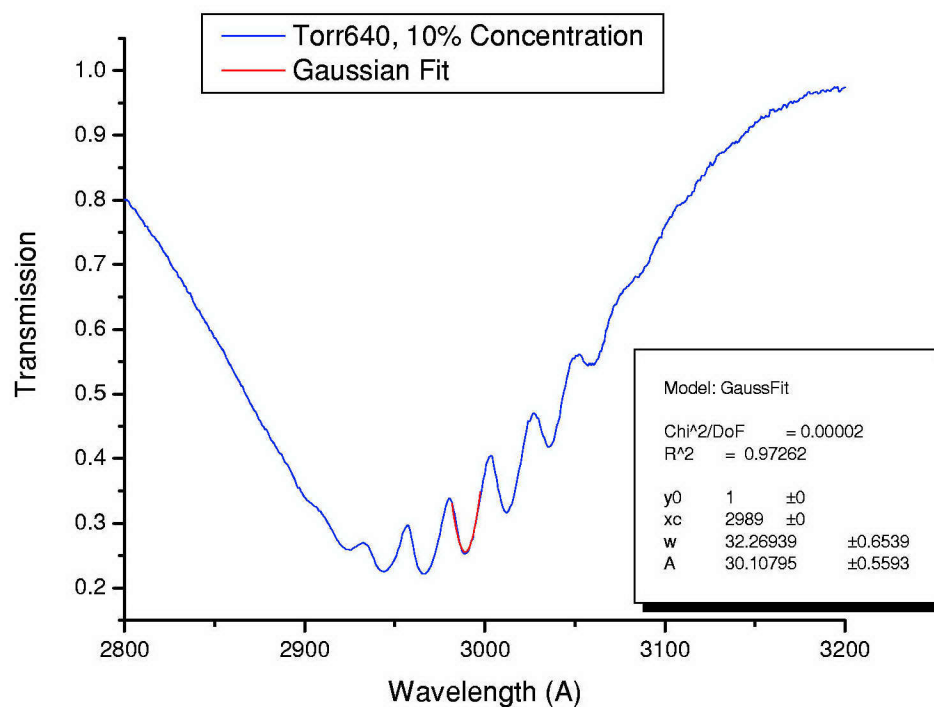
Input Parameters for Curve Fitting

Figure 14.   Sample of the Gaussian Fit using Origin® 6.1 for 10% Concentration and 640 Pressure Torr Dataset for Absorption Line at 2989 Å.

Table 5.   Equivalent Width Obtained From Gaussian Fit

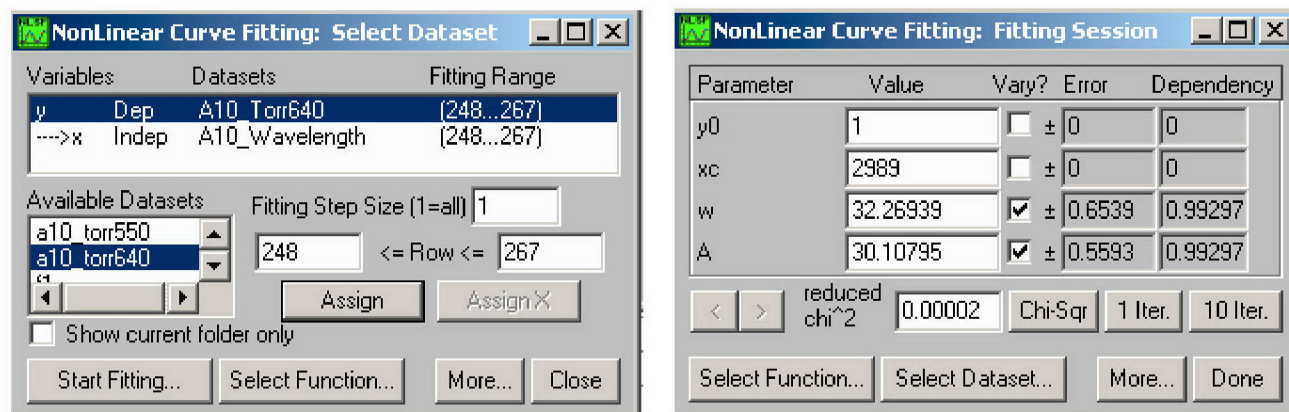| Pressure	Concentration	Molecules/m²	Pixel 200 or λ = 2943Å	Pixel 228 or λ = 2966Å	Pixel 256 or λ = 2989Å	Pixel 256 or λ = 3012Å
550	0.22%	1.284E+21	3.06	2.75	2.30	2.86
275	0.47%	1.378E+21	3.16	2.78	2.59	2.57
640	0.22%	1.494E+21	7.05	5.69	4.76	4.98
365	0.47%	1.829E+21	1.28	1.62	1.43	1.62
185	1.01%	1.991E+21	3.63	3.36	2.99	3.12
450	0.47%	2.255E+21	1.57	1.86	1.76	1.62
550	0.47%	2.756E+21	2.32	2.51	2.33	2.14
275	1.01%	2.959E+21	4.58	4.04	3.49	3.61
640	0.47%	3.207E+21	5.41	4.71	3.69	3.96
365	1.01%	3.928E+21	3.66	3.63	3.01	2.92
185	2.17%	4.275E+21	5.67	4.99	4.16	4.27
450	1.01%	4.842E+21	4.34	4.12	3.45	3.42
550	1.01%	5.918E+21	5.47	4.91	4.14	3.88
275	2.17%	6.354E+21	7.32	6.49	5.32	4.81
640	1.01%	6.887E+21	8.61	7.60	6.25	6.31
365	2.17%	8.434E+21	7.49	6.53	5.55	5.21
185	4.66%	9.179E+21	9.48	8.07	6.83	6.47
450	2.17%	1.040E+22	9.05	8.10	6.55	6.24
550	2.17%	1.271E+22	11.02	9.43	7.75	7.39
275	4.66%	1.364E+22	11.99	10.19	8.43	8.07
640	2.17%	1.479E+22	14.15	11.88	9.69	9.34
365	4.66%	1.811E+22	13.85	11.73	9.62	9.17
185	10.00%	1.971E+22	18.00	14.83	12.24	11.41
450	4.66%	2.233E+22	16.30	13.80	11.27	10.68
550	4.66%	2.729E+22	19.08	16.16	12.95	12.63
275	10.00%	2.930E+22	23.77	18.85	15.49	14.71
640	4.66%	3.176E+22	23.17	18.93	15.38	14.86
365	10.00%	3.889E+22	28.31	22.57	18.19	17.01
450	10.00%	4.794E+22	33.75	26.51	21.54	19.90
550	10.00%	5.860E+22	41.07	32.03	25.58	22.99
640	10.00%	6.819E+22	51.80	38.52	29.77	26.95
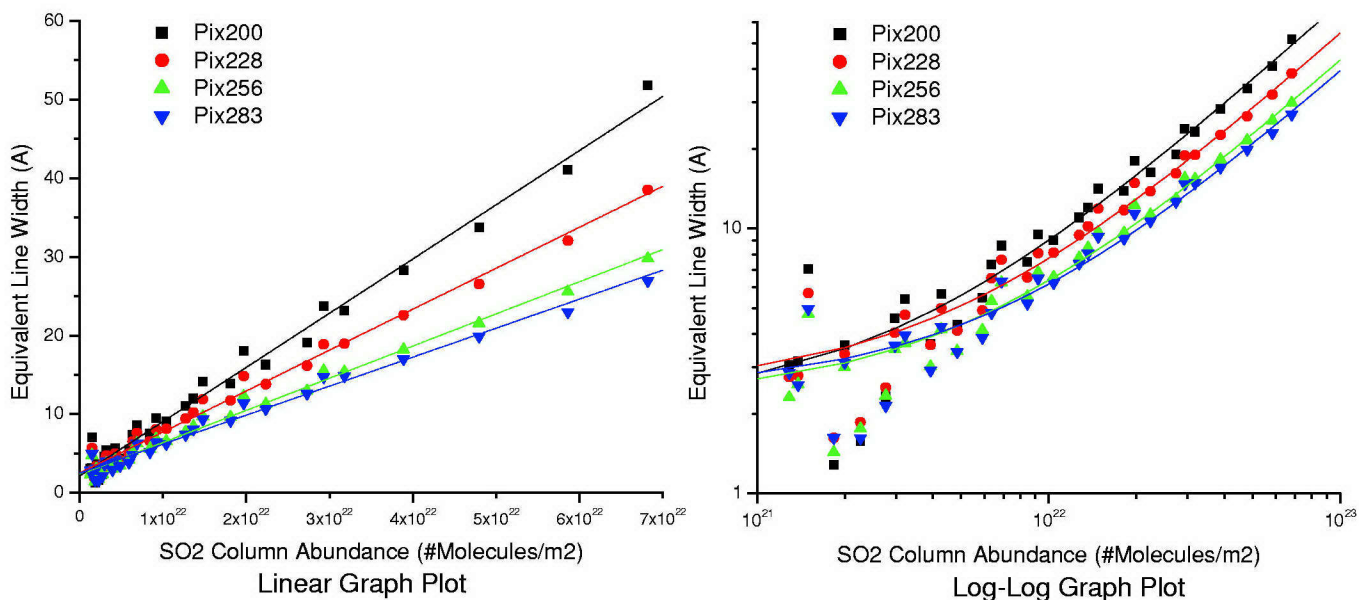
Figure 15. Laboratory Generated Curves of Growth for SO_2

The curves of growth generated seem to give a linear relationship between the equivalent line width and the SO_2 abundance as predicted by the plotted trend lines. The linear fit gives good fidelity only for SO_2 abundance in the range 3×10^{21} to 7×10^{22}. The equations of the trend lines are given in Table 6. The R^2 value indicates the closeness between the actual value and the fitted value and a value of 0.98, or more, can be considered a good fit.

Table 6.   Equation of Trend Lines for Curve of Growth

Trend line for	Linear Equation	Curve Fitting R^2
Pixel 200 or $\lambda = 2943$Å	$Y = 2.15 + 6.894 \times 10^{-22} X$	0.9853
Pixel 228 or $\lambda = 2966$Å	$Y = 2.511 + 5.208 \times 10^{-22} X$	0.9873
Pixel 256 or $\lambda = 2989$Å	$Y = 2.293 + 4.09 \times 10^{-22} X$	0.9860
Pixel 256 or $\lambda = 3012$Å	$Y = 2.488 + 3.688 \times 10^{-22} X$	0.9805

29

THIS PAGE INTENTIONALLY LEFT BLANK

V. OUTDOOR AND FIELD DATA COLLECTION

A. PURPOSE

This chapter describes the outdoor measurement conducted at the roof of NPS Spanagel Hall and near a coal-burning factory at Concord as field samples for data analysis.

B. OUTDOOR ROOF MEASUREMENT

1. LINUS Operational Test

The objective for bringing LINUS up to the roof was to test the operational set up of the equipment for future field measurement. The equipment list includes the LINUS optical system, host control module, mobile generator, LINUS tools set, visibility meter and GPS meter. During the roof test, several problems were encountered which are addressed as good lesson learned.

a. *Mobile Generator*

The mobile generator was tested with the full electrical load switched on to ensure that it has sufficient power for the field test. The generator has a rating of 1kW. It was also important to learn how to use the generator.

b. *Visual Camera*

When the visual camera was operated on the roof, saturation was observed from the monitor screen. The fault was solved easily by adjusting the iris of the telescopic lens to reduce the sunlight exposure. The iris would have to be readjusted when LINUS is used in the laboratory environment. This is a manual adjustment with the optical cover removed.

c. *Functional Test Using the SO₂ Test Cell*

To ensure that LINUS is working properly in the field environment, the SO_2 test cell is placed at the front of entrance aperture. Distinct structural lines can then be observed as a result of SO_2 absorption using the focus mode. This quick test can be used prior to the start of data collection. For the first roof test, the test cell used is a small, enclosed quartz cell of diameter 4 inches and inner path length 3.25 cm from Weiss Scientific Glass Blowing Company. This small test cell was also used for the partial pressure measurement. The test cell was filled with 10% concentration of SO_2 at 1 bar and positive result was concluded from the structures observed. However, this small test cell was accidentally broken while packing up for the first trip to Concord. Another old test cell previously made for NUVIS was used. This old test cell has a diameter of 6 inches and a path length of 12 inches, and filled with 10% concentration of SO_2 at 1 bar. No structural line was observed in the first field measurement and subsequent roof test using this larger test cell. It was then found that the SO_2 abundance was too high with 1 bar pressure and 10% concentration level which absorbed the UV radiation completely. A new test cell was then made by modifying the old test cell with a shorter cylinder to give a shorter path length of 3.5 inches. The pressure was also reduced to 200 torr with the concentration remained at 10%. Structural lines were then observed in the roof test and second field measurement.

2. Verification of Bore-Sight Camera with UV Camera

With the visual camera added into the LINUS system by Cabezas [4], the LINUS operator is able to rotate and tilt the tripod to aim at the target with ease and accuracy. The collected visual images can also be used to compare with the UV camera data for analysis. Cabezas [4] had performed an alignment of the two cameras in the laboratory while installing the visual cameras. He also made an initial verification of the bore-sight of both cameras in the laboratory. The error between the two bore-sights is only minor and the visual camera has a

larger field of view (FOV) to contain the FOV of the UV camera. Two different centers are used as indication to the two cameras line of sights (LOS).

The outdoor measurement at the roof of Spanagel Hall was conducted to verify the bore-sight of the visual camera against the UV camera using a tree as the target image. The visual image was collected using the snap shot button in the LINUS Labview program. The UV image was processed and formed using IDL from the spectra data cube collected as the scanning mirror moved about the azimuth axis. This 2-D UV image had to be clockwise rotated by 90°, flipped horizontally and corrected in aspect ratio to match with the visual image. The visual and UV images are provided in Figure 16. The tree features can be clearly seen in both images and this confirms the verification of the bore-sight of both cameras. By measuring the dimension directly from the picture, the X_{error} and Y_{error} are estimated to be 0.22° and 0.25° respectively.
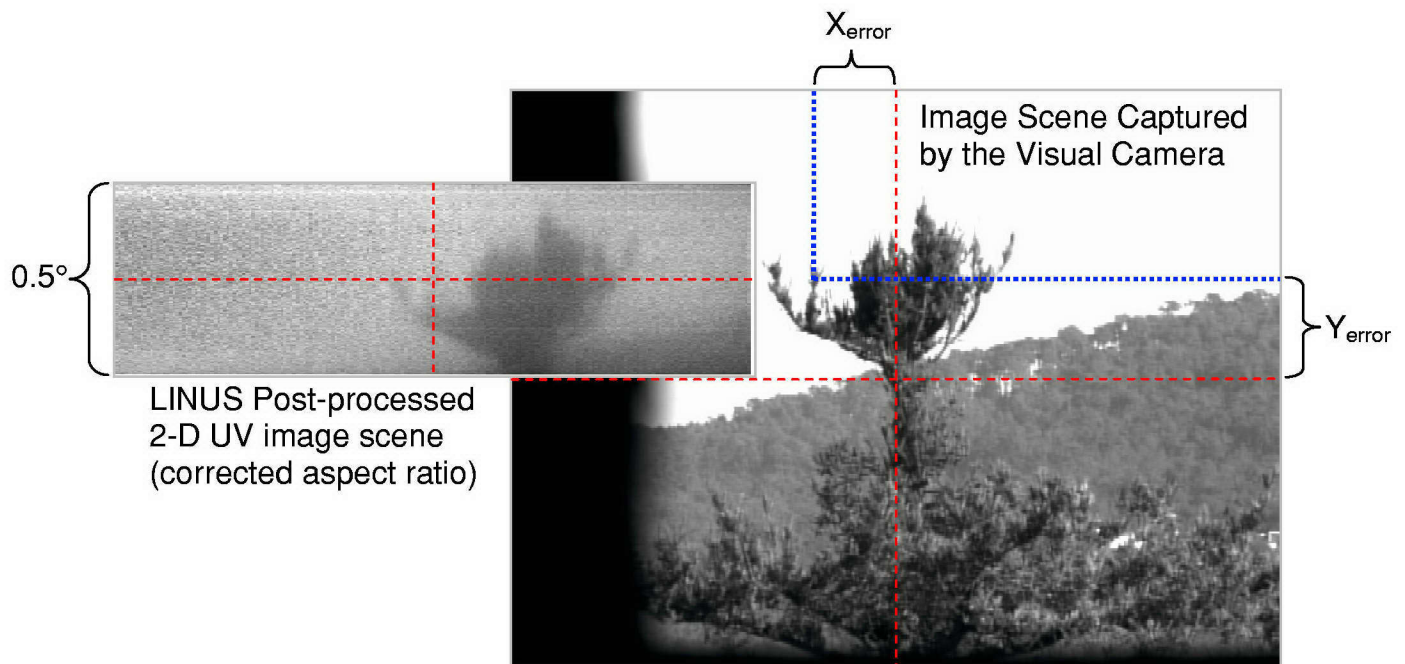

Figure 16. Comparison of Images by Visual Camera and UV Camera

C.   FIELD DATA COLLECTION AT CONCORD

1.   Field Measurement

With LINUS in full operation, the next step was to bring the equipment out to the field for data collection to test its working capability.   The coal-burning factory located near Concord was selected for its reported emission of SO_2 into the atmosphere.   The thick cloud of plumes coming out from its chimneys can be observed at more than ten miles away.   A suitable measurement site at the car park of Calvary Chapel was selected about two miles away with a direct view of the factory. The two locations are plotted on the map shown in Figure 17.   A photograph of the burning factory can be viewed in Figure 18.   The deployment scheme for field data collection is depicted in Figure 19.

Two trips were made on 17 Nov 2004 and 1 Dec 2004. For the first trip, time was spent on surveying to select a good measurement site. Only one data set was made which took more than an hour to capture. The data was analyzed and found no significant information on the presence of SO_2.   Nevertheless, useful experience was gained in deploying LINUS in the field and lessons learned can be applied for follow-on trips.   For the second trip, the time was well spent on data capturing using the same site.   With a team of three, the equipment was set up and deployed quickly.   Twelve useful data sets of different sample sizes were captured during the four hours operation.   The parameters used for the twelve data sets are put in Table 7.
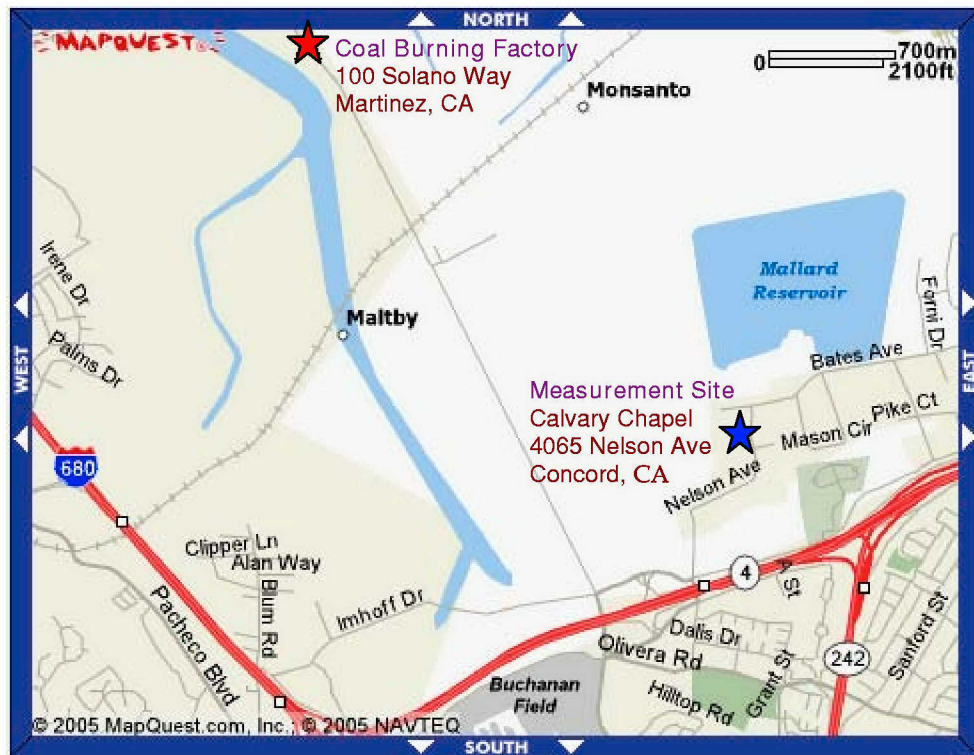
Figure 17. Map Showing the Location of the Coal Burning Factory and the Measurement Site at Concord (After: Map Quest Web Site, Feb 2005 [9])

Figure 18. Digital Camera View of the Coal Factory from the Measuring Site

Figure 19. Equipment Setup for Field Measurement

Table 7.   LINUS Parameters for Second Field Measurement

Filename	Slit width (mm)	MCP (V)	Integration time (s)	Count x steps	Remark
Concord_dc_1	0.2	850	15	1x10	Blue Sky Background with test cell
Concord_dc_2	0.2	850	20	1x10	Blue Sky Background with test cell
Concord_dc_3	0.2	850	20	8x100	Tree Background
Concord_dc_4	0.2	850	5	4x200	Plume stack, factory
Concord_dc_5	0.2	850	5	1x10	Same view as (4) with test cell
Concord_dc_6	0.2	850	10	2x100	Plume stack, factory
Concord_dc_7	0.2	850	15	1x10	Same view as (6) with test cell
Concord_dc_8	0.3	850	16	1x8	Discard data set, mirror position incorrect
Concord_dc_9	0.3	850	16	1x8	Plume stack, factory with test cell
Concord_dc_10	0.3	850	16	1x50	Plume stack, factory, same view as (9)
Concord_dc_11					Dark Current Measurement, MCP off
Concord_dc_12	0.11	850	30	1x10	Discard data set, wrong setting
Concord_dc_13	0.11	850	20	1x10	Blue Sky Background with test cell
Concord_dc_14	0.11	850	20	1x10	Blue Sky Background only
Concord_dc_15	0.11	850	20	1x10	Plume stack, factory

2.   Data Analysis

The Concord 2 data were processed and extracted using the IDL written program called "outdoor.pro". This program reads the input file stored and manipulates the data in array format. The 3-D data is first averaged for the X-component into a 2-D array and displayed using the "TV" command to observe for SO_2 structures. The 2-D array is then averaged for the Y-component into a 1-D vector to observe the structural absorption in a graphical plot. The 1-D vector is exported to Excel for simple analysis and plotting. The related files can be plotted together for direct comparison.

Six of the TV displays are extracted and shown in Figure 20 for illustration. With the test cells inside the LINUS FOV for DC-1, DC-5 and DC-13, clear and distinct structural lines can be seen. Some structures can also be observed with DC-4 to give a strong indication that there may be SO_2 present when the data was captured. On the other hand, no structure was observed for DC-15. Lastly, the display of DC-14 seems abnormal and there is a possibility that the data is saturated. More analysis will be explained in the later section.

Different LINUS parameters were tried in the field measurement, as depicted in Table 7 to collect a variant of data set for analysis. There were a total of 12 useful data sets, which consist of 6 sets with the SO_2 test cell in the optical FOV and another 6 sets with direct measurement of the scene. The results with the test cells are group together and plotted in Figure 21 for comparison. The following were deduced from Figure 21:

a.   Clear & distinct absorption were observed that coincided fairly well for all six samples.

b.   There is a fairly constant level from 2800 to 2970 A which is due to solar absorption by the ozone. The pixel intensity of this level is dependent on the LINUS parameters (slit width, integration time and MCP voltage) and the intensity of the solar radiation during the measurement.

c.   The measurement shows that LINUS is working properly.

37

Similarly, the results without the test cells are plotted in Figure 22 and the following observation are made from this plot.

a. Except for DC-4 and DC-15, the other 4 data sets seem abnormal. There are wide dips in the curves which do not correspond to atmospheric absorption. A view of the 2-D image for DC-14 is given in Figure 20 where the wide dip corresponds to the "dark" area. No good explanation is given for this observation. However, by analyzing the LINUS parameters for these 6 sets, DC-4 had the lowest integration time. Although DC-15 shared the same parameters as DC-14, its view of the factory had a lower solar radiation. The peak DN value for DC-15 is still high. Thus, a lower integration time around 5 to 10 sec may be a better choice to avoid saturation for future field measurement. The parameters cannot be compared with the 6 sets with test cell due to the attenuation of the quartz window and SO_2.

b. Similar conclusion made from the TV display in Figure 20 for DC-4 and DC-15 is given here. There is a good indication for traces of SO_2 in DC-4 data set but not in DC-15. However, the absorption lines for DC-4 are not as distinct as compare to the cases with the test cells in the FOV.
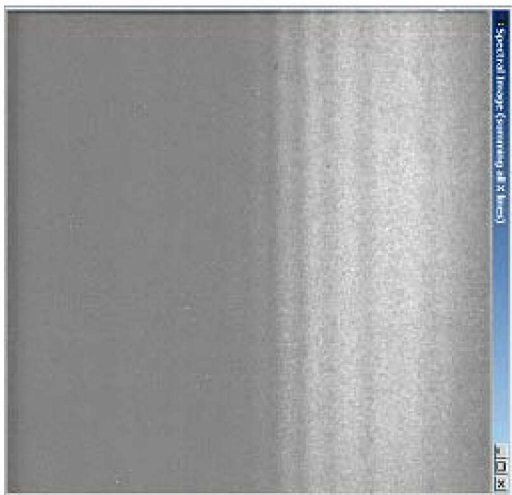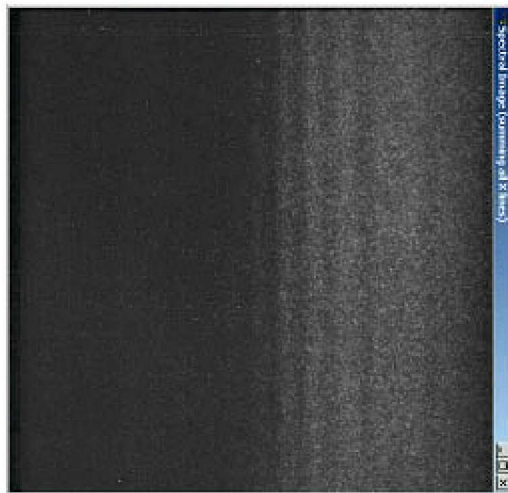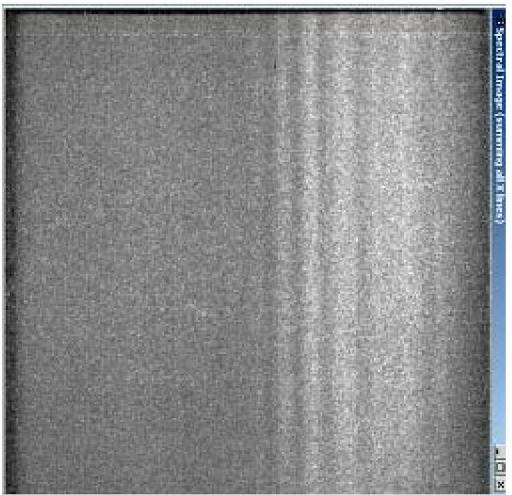
DC1 – blue sky with test cell
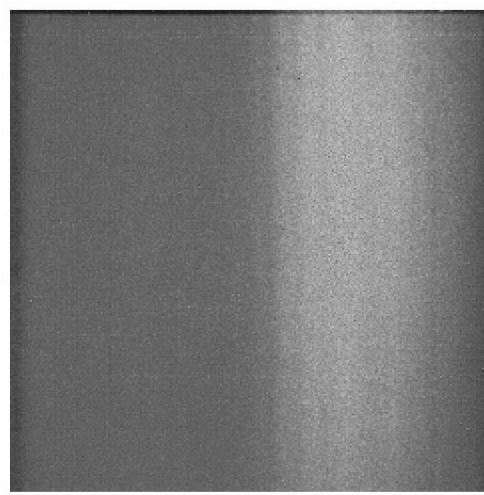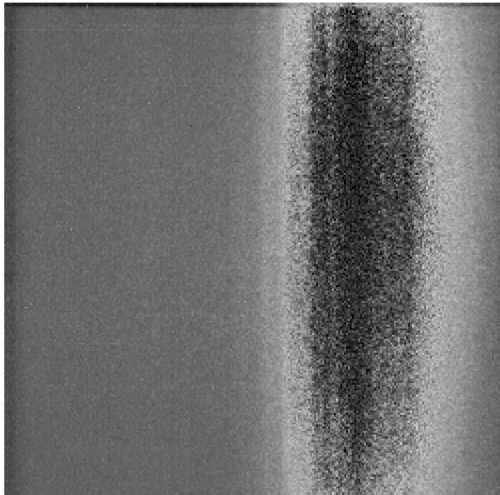

DC 15 – plume stack
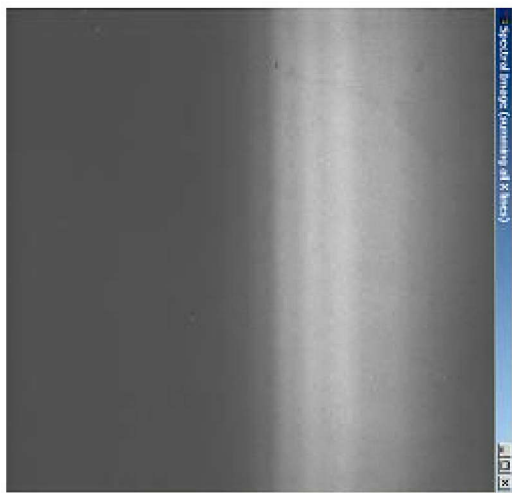
DC4 – plume stack

DC 5 – plume stack with test cell

DC13 – blue sky with test cell

DC 14 – blue sky

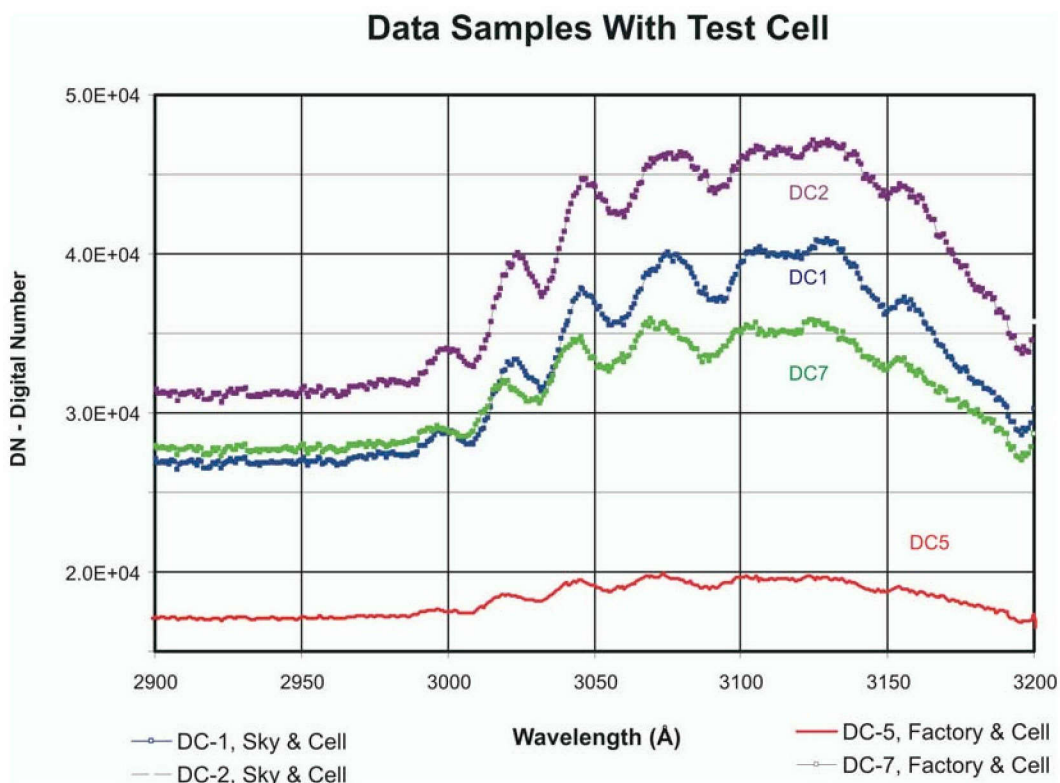Figure 20.   IDL TV Displays for Concord data

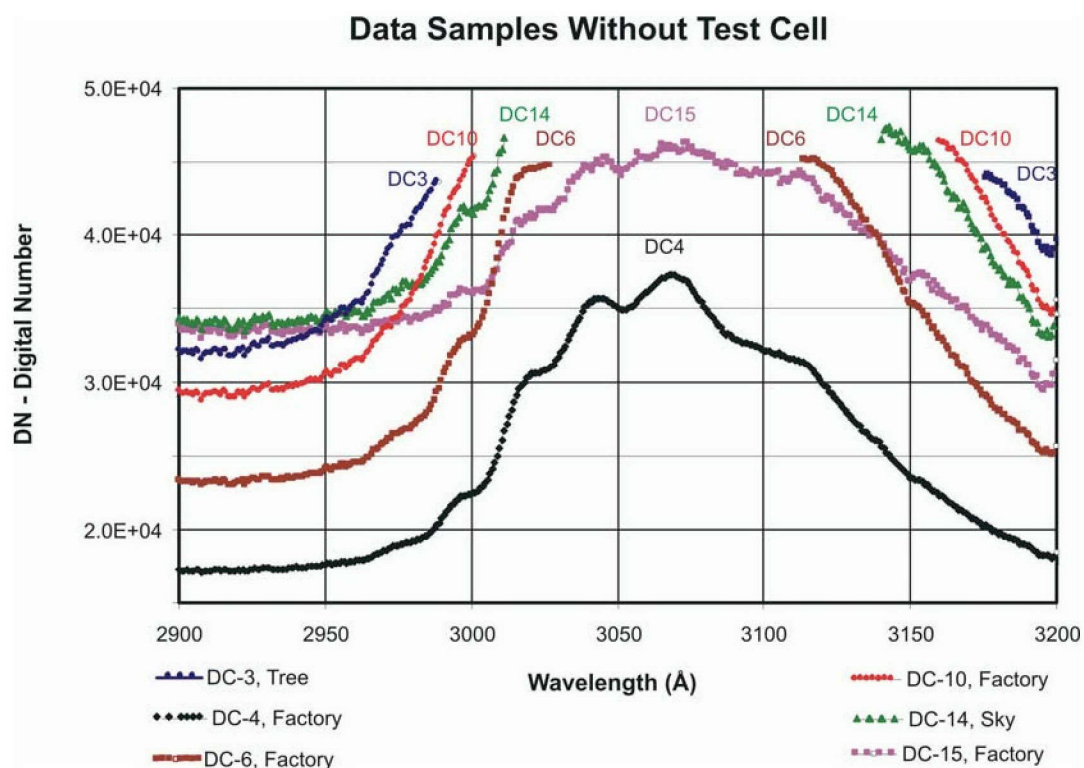Figure 21. Data Samples with SO_2 Test Cell in FOV

Figure 22. Data Samples without SO_2 Test Cell in FOV

40
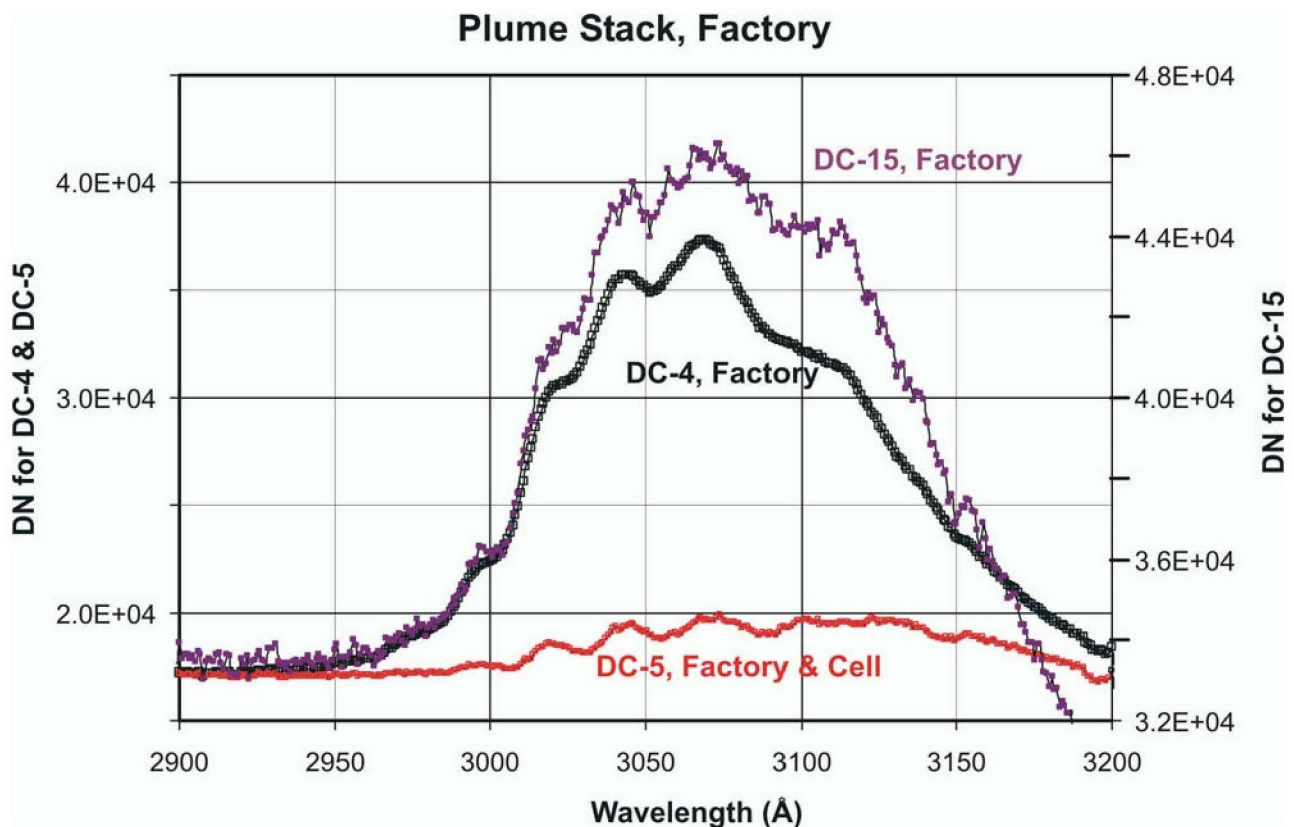
Figure 23. Comparison between DC-4, DC-5 and DC-15 Samples

Finally, a comparison of data sets for DC-4, DC-5 and DC-15 are plotted in Figure 23.   DC-4 and DC-5 were of the exact same scene with the same LINUS parameter. Their only difference is the test cell in the FOV for DC-5. The absorption centers show good match by coinciding with one another. The peak DN value for DC-5 dropped drastically due to the addition of the test cell. The DN value for DC-15 (reading from the secondary axis on the right of the plot) is much higher than DC-4 & 5 due to the long integration time.

DC-15 also corresponds to a factory scene measurement but differs in aiming location with DC-4 & 5 as shown in Figure 24. This explains why there is no SO_2 structure in DC-15 TV image but in DC-4 TV image. It is possible that only the chimneys in DC-4 data were operating to produce the smoke stacks with SO_2.

41

In conclusion, SO_2 is detected in the data set DC-4 for the Concord field measurement. It is quite tedious to make an analysis using the experimental curves of growth to determine the abundance level as there is no good clear sky data for comparison. The clear sky measurement looks to be saturated. Further tests should focus on capturing more data without the test cell and with a shorter integration time.
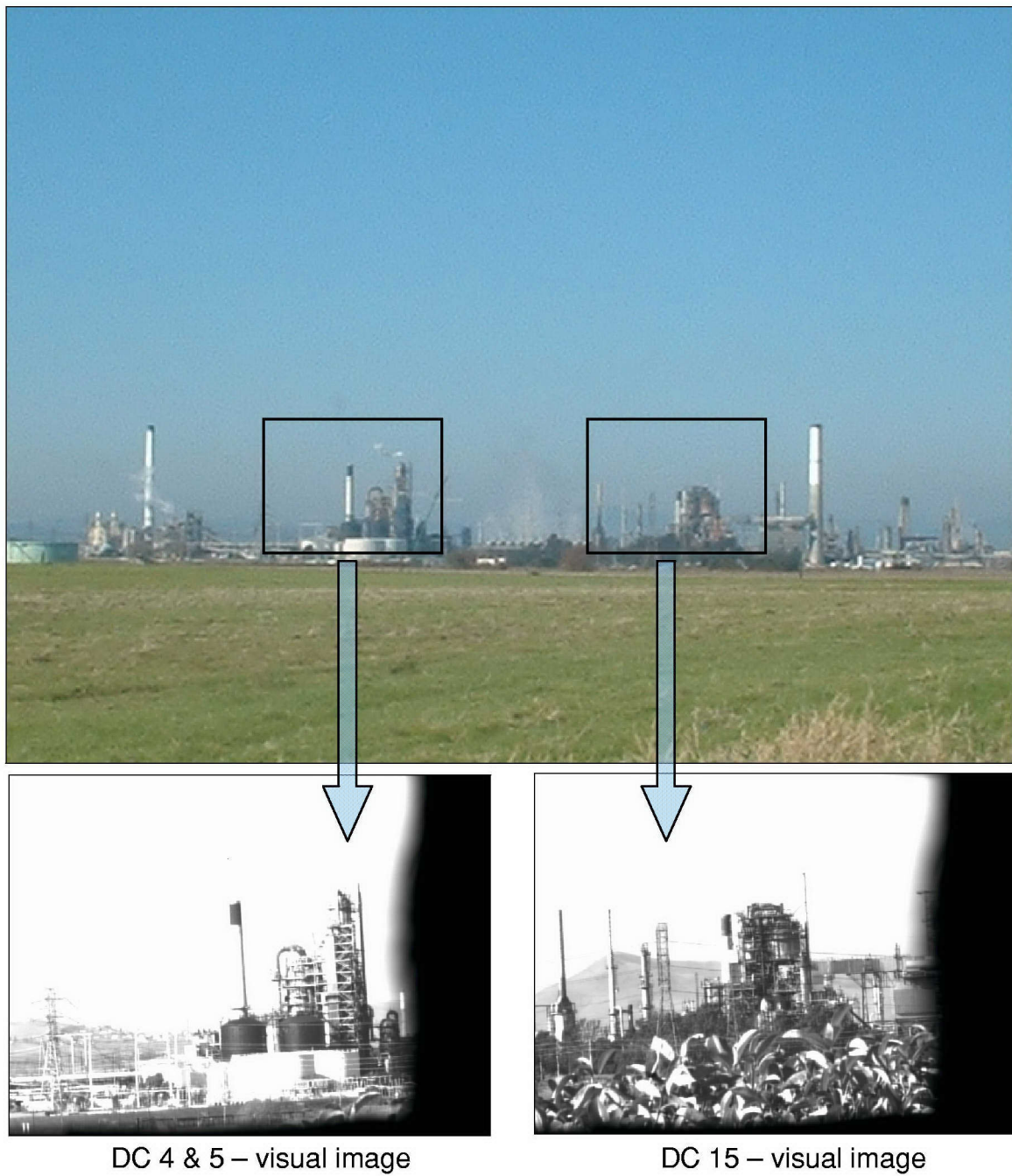
DC 4 & 5 – visual image   DC 15 – visual image

Figure 24. Comparison Between Visual Images for DC-4 and DC-15 Data

THIS PAGE INTENTIONALLY LEFT BLANK

VI. CONCLUSION AND RECOMMENDATIONS

A. CONCLUSION

This project had completed the laboratory experiments for the partial pressure measurement and obtained the curve of growth for the SO_2 absorption profile. LINUS had successfully acquired SO_2 data for the field test against a man-made source from a coal-burning factory. The visual camera was verified and used in the field as a good bore-sighting tool for LINUS to aim and capture the target image. In the past, it would take a team of more than four persons to deploy LINUS in the field. In the two Concord trips, LINUS was deployed with just a team of three persons and the set up time is around 20 minutes.

B. RECOMMENDATIONS

The follow-on work for LINUS is to conduct more field tests against man-made (coal factories) and natural sources (volcanoes) of SO_2. From the small traces of SO_2 observed, it is still worthy to plan another trip to the same site at Concord to conduct further testing. The Concord location is only 2 hours drive from Monterey and the measurement can be concluded in a day. Other possible locations may require more than 10 to 20 hours of driving to reach and the whole trip would take about 3 to 5 days.

The LINUS project still needs a boost in confidence with good SO_2 data from field measurements to prove its capability. This requires a good location where a strong abundance of SO_2 can be ascertained to carry out the measurement trip. It is known that active volcano would produce lots of SO_2, but to conduct a measurement near it may be high risk. For non-active volcano, the SO_2 produced is undetermined.

THIS PAGE INTENTIONALLY LEFT BLANK

APPENDIX A: START UP, SHUT DOWN AND OPERATING PROCEDURE FOR LINUS

START UP PROCEDURE

a) Connect the cables from the controller module to the camera module as labeled on each cable.

b) Ensure that all switches are set to the "OFF" position before switching on the "MAIN" power supply located at the back of the controller module. Ensure also that the MCP (micro channel plate) power switch located at the back panel of the Pulse Generator is switched "OFF".

c) Turn "ON" the "MAIN" power supply and then turn on the Host Computer. Wait till the Windows is successfully booted.

d) Turn "ON" the Camera Temperature Controller with its power switch located at the back. Turn "ON" the temperature control located at the front panel. The norm temperature setting is –25.6°C.

e) Turn "ON" the Power Amplifier which controls the scanning mirror for LINUS. Turn "ON" the Enable switch also.

f) Turn "ON" the Pulse Generator with its switch located at the back. Refer to the manual of the Pulse Generator for detailed operation. To just change the MCP voltage, press "Func" and "77". Then key in the required voltage and press "Enter". The MCP voltage is still not supplied to the camera unless the MCP Power switch located at the back panel is turn "ON". Only turn "ON" this MCP Power switch when you are ready to measure in the UV spectrum.

g) Run the Labview program LINUS located at the desktop of the screen by double click the icon. Then click the arrow button [⇨] at the top left corner of the window to run the LINUS program. When the program is loaded, go to "Manual Control" page and click the "Initialize" button. Then click the "Go to Bore Sight" button. Now, check that the scanning mirror is at bore-

sight position by looking into the entrance aperture of LINUS; you should be seeing your own image. Click the "Camera Settings" button. It will bring up a new page call Controller Status. Click "Done" to return and the display "UV Camera Status" should turn from red to green. The software is now initialized and ready for operation.

SOFTWARE OPERATING PROCEDURE

a)   To observe the UV spectrum, turn "ON" the MCP switch located at the back of the Pulse Generator. You should hear one "beep" sound indicating the hardware is working properly. If there is more than one "beep" sound, immediately switch "OFF" the MCP switch and the Pulse Generator. Refer to the manual for further assistance.

b)   Click on the "Go To Collimate" to move the scanning mirror such that the UV Camera is viewing at the centre of the entrance aperture.   The collimate position corresponds to Motor Position of 12965 or Mirror Angle of 0°. Click on the "Focus" button and the UV spectrum will appear on a new window. The "Snap" button when pressed will store a JPEG image of the UV spectrum at present motor position onto the directory C:\A_Linus\data using the format "yyyymmddhhmmss" (corresponding to year|month|day|hour|minute|second) as the file name. Intuitively, "Snap At Collimate" is to store the UV image at collimate position. Click on the "Camera Settings", then "Acquisition Setup" for changing the "Integration Time" when needed. Click "Overwrite Defaults" to save your changes and then click "Done" to exit. Do no change any other settings in this menu without knowing its purpose.

c)   Click on "Aiming Control" page. Click on "Align Cameras". A visual image is displayed in a new window. The scanning mirror automatically moves to the correct position for the CCD camera to view through the LINUS aperture. Click "Stop" to exit. To store a snapshot of this visual image, click "Aiming LINUS" followed by the "SNAP" button in the new window.

48

Click "Done" to exit. (Note: the system may "hang" occasionally at this stage due to instability of the program; sometimes, it may recover by clicking onto another window). The image is stored similarly to Step b) above. This visual image can later be compared with the X-Y image for the UV spectrum after processing. (Note: the aspect ratio of the UV image may have to be corrected through translation depending on the number of scanned lines in order to match with the visual image.

d)   To make a recording, go to the "Scan Control" page. Depending on the number of scan frames, enter the values for Starting Absolute Position, Counts/Step and Steps. For e.g., with the collimate or center position = 12965, with a Count/Step = 4, and Steps = 200, then Starting Absolute Position = 12965 + ½*200*4 = 13365. A total of 200 images will then be recorded which span from 12565 to 13365 with its center frame at 12965 at a space interval of 4 steps.

e)   Click "Change Filepath" button to change the filename. To change the stored directory, click the "Change Directory" button. Click "Done" to exit.

f)   To start the recording sequence, click the "Start Scan button. An estimated scan time needed is computed and displayed. The progress of this job is also displayed. An outdoor measurement for an Integration Time of 15 seconds and a total of 200 frames will take about 50 minutes.

g)   Do not change any other settings without knowing its purpose. Consult the professors when in doubt.

SHUT DOWN PROCEDURE

a)   Turn "OFF" the MCP power switch when the UV camera is not needed.

b)   To shut down, first turn "OFF" the "Enable" switch followed by the "AC Power" switch for the Power Amplifier. This is to prevent the scanning mirror from moving erratically when the Host Computer is shut down.

c) Click the "Exit" button. Close the window for the Labview program and shut down the host computer.

d) Turn "OFF" the Temperature Control for the Camera Temperature Controller. Then turn "OFF" the power switch at the back panel.

e) Turn "OFF" the power switch at the back panel of the Pulse Generator.

f) Lastly, turn "OFF" the Main switch for the Controller Module.

APPENDIX B: PROCEDURE FOR PARTIAL PRESSURE MEASUREMENT

a)   Turn down the regulators for both tanks to the lowest. Turn on the opening valves (not in diagram) for both tanks. Increase the regulator pressure to 20 psi for both tanks.

b)   Turn on taps A, B, E, F, G, H, and I. Switch on the power for the vacuum pump. Turn on tap J. Allow the pressure to decrease to 0 mm Hg by reading from the pressure gauge. Turn off tap J. Switch off the power for the vacuum pump.

c)   Collect the LINUS data for the Test Cell in vacuum.

d)   Switch off tap G and H. Turn on tap C slowly to allow 10% volume of SO_2 gas to enter into Chamber I and II until a pressure of 500 mm Hg is reached and turn off tap C. Keep the concentration in Chamber I by turning off tap A. Turn on tap G to allow the SO_2 gas to flow to the Test Cell. Record down the new reduced pressure ($\approx$ 450 mm Hg). Collect the LINUS data for the Test Cell filled with 10% volume of SO_2 gas.

e)   Switch on the power for the vacuum pump. Turn on tap J. Allow the pressure to decrease to 0 mm Hg then turn off tap J. Switch off the power for the vacuum pump. Turn off tap G.

f)   Turn on tap A. Allow the volume of SO_2 gas in Chamber I to be transferred to vacuumed Chamber II. The 2 chambers now have equal portion of SO_2 due to their equal in volume. The pressure should drop slightly below 250 mm Hg due to the pipelines.

g)   Turn on tap D slightly to fill up the tube to tap H. Then slowly turn on tap H to fill up the 2 chambers with N_2 gas till the pressure of 500 mm Hg is reached and turn off tap H and tap D. The concentration of SO_2 in both chambers is now reduced by half as compare to the original Chamber I

51

before mixing (Step 6). Maintain the new concentration in Chamber I by turning off tap A.

h)   Turn on tap G to allow the SO_2 gas to flow to the Test Cell. Record down the new reduced pressure ($\approx$ 450 mm Hg). Collect the LINUS data for the Test Cell filled with 5% volume of SO_2 gas.

i)   Repeat Steps 5 to 8. For each repeat cycle, the collected LINUS data corresponds to a half reduction in volume of SO_2 gas from the previous cycle. Repeat this process until there is no longer any observation of SO_2 absorption lines from LINUS (use focus mode to observe).
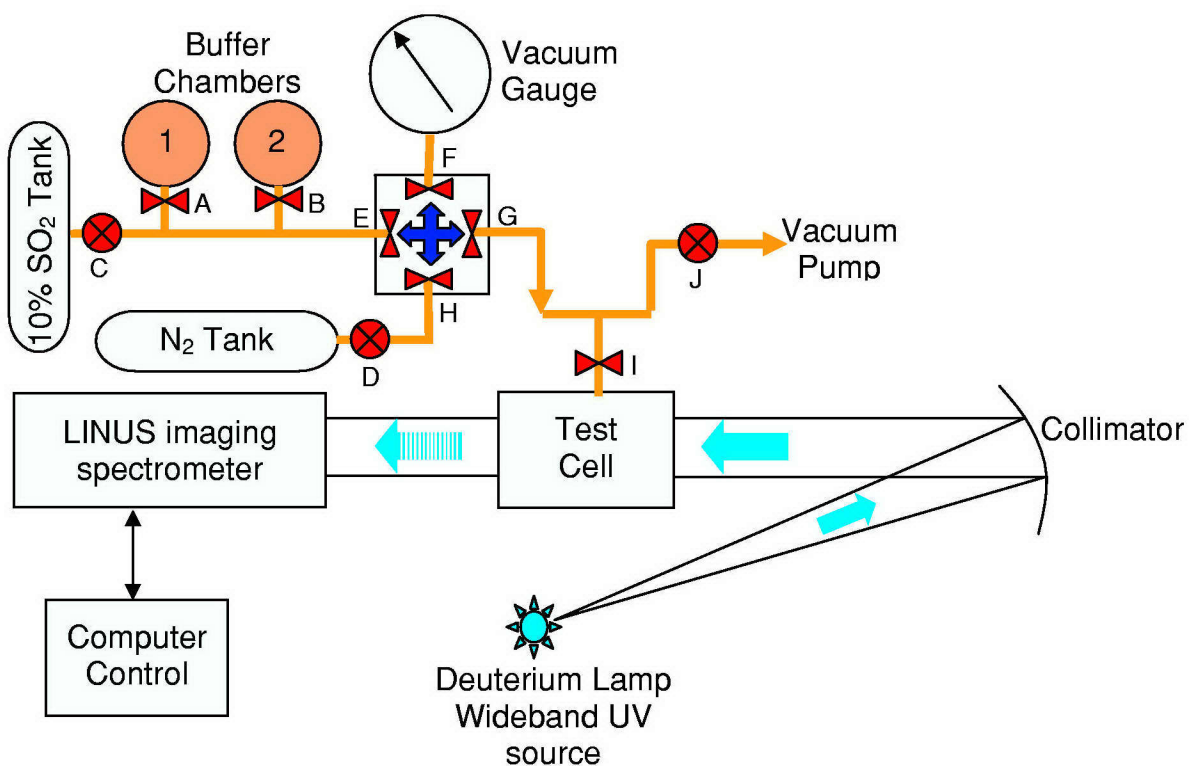

Figure 25. Schematic Diagram for Partial Pressure Measurement

LIST OF REFERENCES

[1]   Kompatzhi, R.C., "Design And Development Of The Image Scanner For Lineate Imaging Near Ultraviolet Spectrometer (LINUS)", Master Thesis, Naval Postgraduate School, Monterey California, December 2000

[2]   Gray, J, "Design and First Operations of the Lineate Image Near Ultraviolet Spectrometer (LINUS)", Master Thesis, Naval Postgraduate School, Monterey California, December 2002

[3]   Halvatzis, A.G., "Passive Detection of Gases In The Atmosphere. Case Study: Remote Sensing of SO_2 In The UV Using LINUS", Master Thesis, Naval Postgraduate School, Monterey California, December 2002

[4]   Cabezas, R, "Design of a Bore Sight Camera for the Lineate Image Near Ultraviolet Spectrometer (LINUS)", Master Thesis, Naval Postgraduate School, Monterey California, June 2004

[5]   Pedrotti, F.L., Pedrotti, L.S., "Introduction to Optics", Second Edition, Prentice Hall, 1993

[6]   Davis, S.C., Harkins, R.M., Olsen, R.C., "The LINUS UV Imaging Spectrometer", Proceedings of SPIE 5093, pp 748-757, 2003.

[7]   Marino, S.A., "Operation and Calibration of the NPS Ultraviolet Imaging Spectrometer (NUVIS) in the Detection of Sulfur Dioxide Plumes", Master Thesis, Naval Postgraduate School, Monterey California, December 1999

[8]   "Encyclopedia of Volcanoes", Academic Press, 2000

[9]   MapQuest Web Site, Feb 2005.

THIS PAGE INTENTIONALLY LEFT BLANK

INITIAL DISTRIBUTION LIST

1. Defense Technical Information Center
   Ft. Belvoir, Virginia

2. Dudley Knox Library
   Naval Postgraduate School
   Monterey, California

3. Richard C. Olsen, Code PH OS
   Naval Postgraduate School
   Monterey, California

4. Richard Harkins, Code PH HK
   Naval Postgraduate School
   Monterey, California

5. Dan Boger, Code IS
   Naval Postgraduate School
   Monterey, California

6. Sing Soong Khoo
   DSO National Laboratories
   Singapore